

1 **The potential of paludiculture for reducing GHG emissions and**  
2 **the importance of heterogeneity in rewetting fen peatlands**

3 **Andres F. Rodriguez<sup>1</sup>, Johannes W.M. Pullens<sup>1,2</sup>, Jesper R. Christiansen<sup>3</sup>, Klaus S.**  
4 **Larsen<sup>3</sup>, and Poul E. Lærke<sup>1,2</sup>**

5 <sup>1</sup> Department of Agroecology, Aarhus University, Tjele, 8830, Denmark

6 <sup>2</sup> iCLIMATE Interdisciplinary Centre for Climate Change, Aarhus University, Roskilde,  
7 4000, Denmark

8 <sup>3</sup> Department of Geosciences and Natural Resource Management, University of Copenhagen,  
9 Copenhagen, 1958, Denmark

10

11 *Correspondence to:* Andres F. Rodriguez (afrodriguez@agro.au.dk)

12 **Abstract**

13 Rewetting drained peatlands can reduce CO<sub>2</sub> emissions but prevents traditional agriculture.  
14 Crop production under rewetted conditions may continue with flood-tolerant crops in  
15 paludiculture, but its effects on greenhouse gas (GHG) emissions compared to rewetting  
16 without further management are largely unknown. This study was conducted between 2021  
17 and 2022 on a fen peatland in central Denmark established with Reed Canary Grass (RCG) in  
18 2018. Three harvest/fertilization management treatments (0, 2, and 5-cut) were applied with  
19 the 2-cut and 5-cut treatments receiving 200 kg N ha<sup>-1</sup> y<sup>-1</sup> in equal split doses, whereas the 0-  
20 cut remained unfertilized. Measurements of CO<sub>2</sub> and CH<sub>4</sub> emissions were conducted  
21 biweekly under four different light intensities using a manual chamber connected to a gas  
22 analyzer. Although the mean annual water table depth (WTD) was -8 cm, indicating a rather

23 wet peatland, the site remained a CO<sub>2</sub> source with a mean net ecosystem C balance of CO<sub>2</sub>  
24 (NECB) of 6.5 t C ha<sup>-1</sup> yr<sup>-1</sup> across treatments. Results showed that management marginally  
25 increased biomass production reflected by more negative gross primary productivity (GPP) in  
26 2-cut and 5-cut compared to 0-cut. No significant treatment effect was found on NECB, but  
27 the interaction between block and treatment indicated that biomass harvest in comparison  
28 with no management, might potentially reduce GHG emissions from the more productive  
29 peatland area, whereas on the less productive area it might be beneficial to leave the biomass  
30 unmanaged. Model simulation of ecosystem respiration (R<sub>eco</sub>) using WTD data of high  
31 temporal resolution captured the variability better as compared to the use of mean annual  
32 WTD, which underestimated R<sub>eco</sub> by 18% on average compared to the hourly WTD model.  
33 Data on pore water chemistry further improved statistical linear models of CO<sub>2</sub> fluxes using  
34 soil temperature (Ts), WTD, ratio vegetation index (RVI) and photosynthetic active radiation  
35 (PAR) as explanatory variables. Significant differences in CO<sub>2</sub> emissions and water chemistry  
36 parameters were found between studied blocks, with higher R<sub>eco</sub> corresponding to blocks  
37 where higher pore water nutrient concentrations were present. Methane emissions averaged  
38 113 kg of CH<sub>4</sub> ha<sup>-1</sup> yr<sup>-1</sup>, equivalent to 11.3% of the total net carbon emission given as CO<sub>2</sub>  
39 equivalents. Overall, the study found that paludiculture allowed the production of a biomass  
40 resource in a rewetting agricultural peatland without increasing the carbon footprint  
41 compared to no management activity.

## 42 **1 Introduction**

43 Peatlands are an essential component of the global carbon (C) cycle. Covering only 3% of the  
44 terrestrial surface they store ~600 Gt of C, equivalent to 30% of the global soil C pool and  
45 exceeding the C stored in vegetation by ~150 Gt (Yu et al., 2010; Scharlemann et al., 2014;  
46 Erb et al., 2018; Leifeld and Menichetti, 2018). Northern temperate peatlands can be

47 classified as bogs or fens and store 21.9 Gt C (Leifeld and Menichetti, 2018). While bogs are  
48 rain fed and nutrient poor, fens receive drain and ground water from the upland and  
49 occasionally from the streams under flooding conditions, making them minerotrophic with a  
50 pH close to neutral because the incoming waters carry minerals released from surrounding  
51 soils and sediments. Under high nutrient concentrations, fens are dominated by grasses and  
52 sedges such as *Phragmites* sp. and *Cladium* sp. (Page and Baird, 2016; Kreyling et al., 2021).

53 Peatland drainage creates aerobic conditions leading to peat mineralization, and consequently  
54 soil C is emitted as CO<sub>2</sub> to the atmosphere (Page and Baird, 2016), and dissolved C and N  
55 compounds are leached from the soil (Cabezas et al., 2012; Liu et al., 2019). Emissions from  
56 drained peatlands are estimated globally to 785 Mt CO<sub>2</sub> equivalents and the water table is  
57 considered the main controlling factor (Zhong et al., 2020; Evans et al., 2021) with higher  
58 water tables resulting in lower CO<sub>2</sub> emissions (Tiemeyer et al., 2020; Evans et al., 2021;  
59 Koch et al., 2023). However, other factors such as soil temperature (Ts), vegetation, and  
60 nutrient status may also affect CO<sub>2</sub> emissions from drained peat soils (Wilson et al., 2016;  
61 Rigney et al., 2018; Bockermann et al., 2024). While rewetting reduces CO<sub>2</sub> emissions, it  
62 may also lead to increased CH<sub>4</sub> emissions (Wilson et al., 2016; Zhong et al., 2020; Darusman  
63 et al., 2023). The CO<sub>2</sub> / CH<sub>4</sub> emission trade-off depends on the water table, the origin of the  
64 water (bog/fen), type of vegetation (Rigney et al., 2018; Purre et al., 2019), its nutrient status  
65 (Wilson et al., 2016; Tiemeyer et al., 2020), as well as gradual changes in the microbial  
66 community following rewetting (Putkinen et al., 2018; Hemes et al., 2019; Emsens et al.,  
67 2020; Urbanova and Barta, 2020); However, even considering temporary increases in CH<sub>4</sub>  
68 emissions, peatland rewetting and restoration leads to the reestablishment of the C sink  
69 function of these ecosystems (Leifeld et al., 2019; Loisel and Gallego-Sala, 2022). Upon  
70 drainage, degradation of peat soils is manifested by increases in peat bulk density (Liu et al.,  
71 2019; Loisel and Gallego-Sala, 2022), and peat chemistry changes leading to decreasing C:N

72 ratio, humic compounds, and polyphenols, while dissolved organic C (DOC) and N (DON)  
73 increase, these changes in peat chemistry may in turn enhance organic matter mineralization  
74 (Cabezas et al., 2012; Liu et al., 2019; Zak et al., 2019), and the release of nutrients along  
75 with higher bacterial and fungal activity increases CO<sub>2</sub> emissions (AminiTabrizi et al., 2022;  
76 Song et al., 2022).

77

78 The importance of peatlands for C storage and GHG emission mitigation, as well as other  
79 environmental services, has sparked an interest in peatland restoration with focus on  
80 rewetting (Page and Baird, 2016; Andersen et al., 2017). Rewetting can be achieved through  
81 different pathways depending on the land use in the peatland after raising the water table.  
82 Peatlands have often been rewetted without altering the already established plant community  
83 or with the attempt to reestablish the native plant community. Paludiculture has been  
84 suggested as an alternative land use, enabling continued agricultural biomass production on  
85 the rewetted peatlands under low or high management intensity (Tanneberger et al., 2020;  
86 Ziegler, 2020). Paludiculture is expected to reduce CO<sub>2</sub> emissions due to the water-saturated  
87 conditions of the peat soils (Ren et al., 2019; Tanneberger et al., 2020; De Jong et al., 2021)  
88 while producing biomass for renewable energy such as biogas production (Dragoni et al.,  
89 2017; Ren et al., 2019; Hartung et al., 2020) or insulation material that can be used as a green  
90 alternative in the building industry (De Jong et al., 2021). Paludiculture may also have the  
91 potential to remove excess nutrients from rewetted peatlands by nutrient removal with the  
92 harvested biomass (Giannini et al., 2017; Vroom et al., 2018; Geurts et al., 2020).

93 Large variation in quantified annual GHG emission from different land use of rewetted  
94 peatlands including paludiculture have been reported and further studies are needed to  
95 establish emission factors accordingly (Bianchi et al., 2021). It is well accepted that GHGs

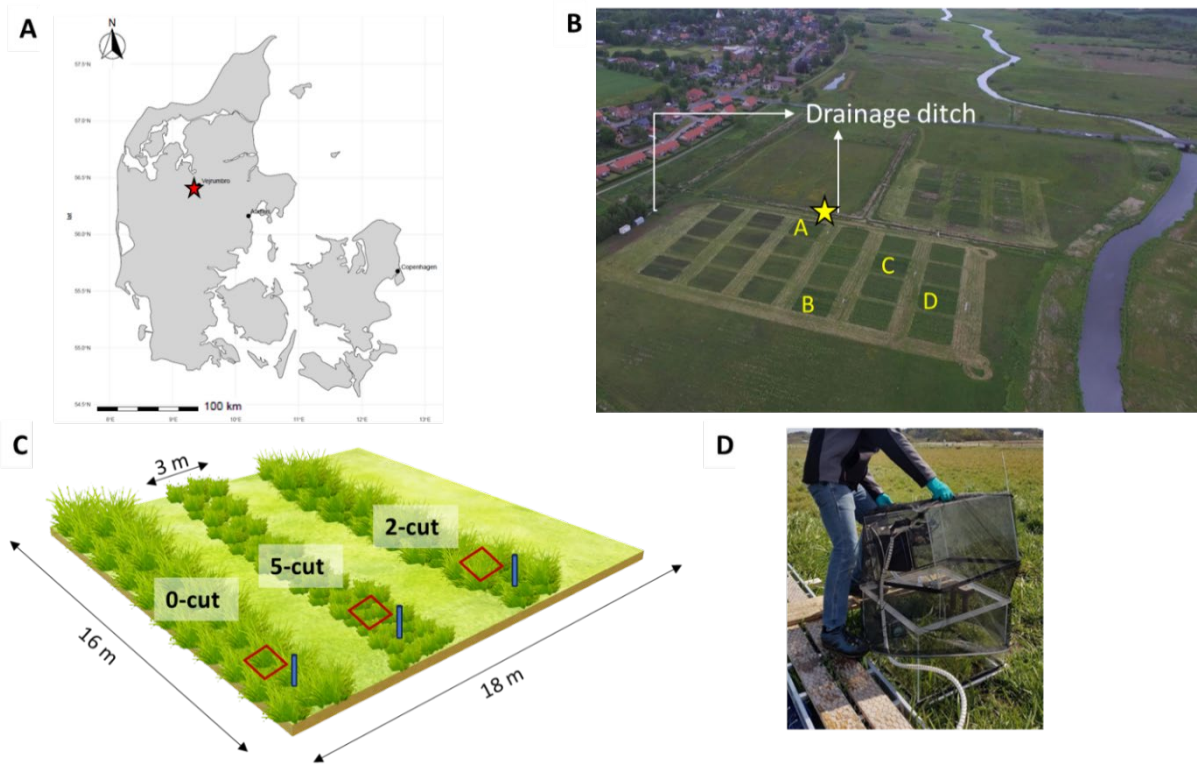
96 from rewetted peatlands are influenced by their nutrient content and water table level,  
97 reflected by IPCC Tier 1 emissions factors (Wilson et al., 2016). Mean annual water table  
98 depth has also been used to predict the net ecosystem carbon balance (NECB), but much  
99 uncertainty remains (Tiemeyer et al., 2020; Evans et al., 2021; Koch et al., 2023). The  
100 complexity and temporal resolution of gap filling models can also influence the NECB  
101 estimates (Karki et al., 2019; Liu et al., 2022) and it is highly uncertain how different  
102 management practices, water table dynamics during the year, and nutrient status affect annual  
103 emission budgets. Consequently, the objectives of this study were to: (1) determine the CO<sub>2</sub>  
104 NECB of reed canary grass (RCG) production under three harvest and fertilization  
105 management regimes during the third year after establishment in a fen peatland with shallow  
106 WTD, (2) assess model performances in gap filling biweekly measurements of ecosystem  
107 respiration ( $R_{eco}$ ) and gross primary productivity (GPP), and (3) investigate the relation of  
108 soil water chemistry with  $R_{eco}$  and GPP. We hypothesized that, (a) fertilization and harvest of  
109 RCG would increase C emissions compared to no RCG management, (b) use of high-  
110 temporal frequency data on water table depth (WTD) would improve model prediction of  
111 ecosystem respiration ( $R_{eco}$ ), and (c) knowledge on soil pore water chemistry would improve  
112 explanation of C fluxes.

## 113 **2 Materials and methods**

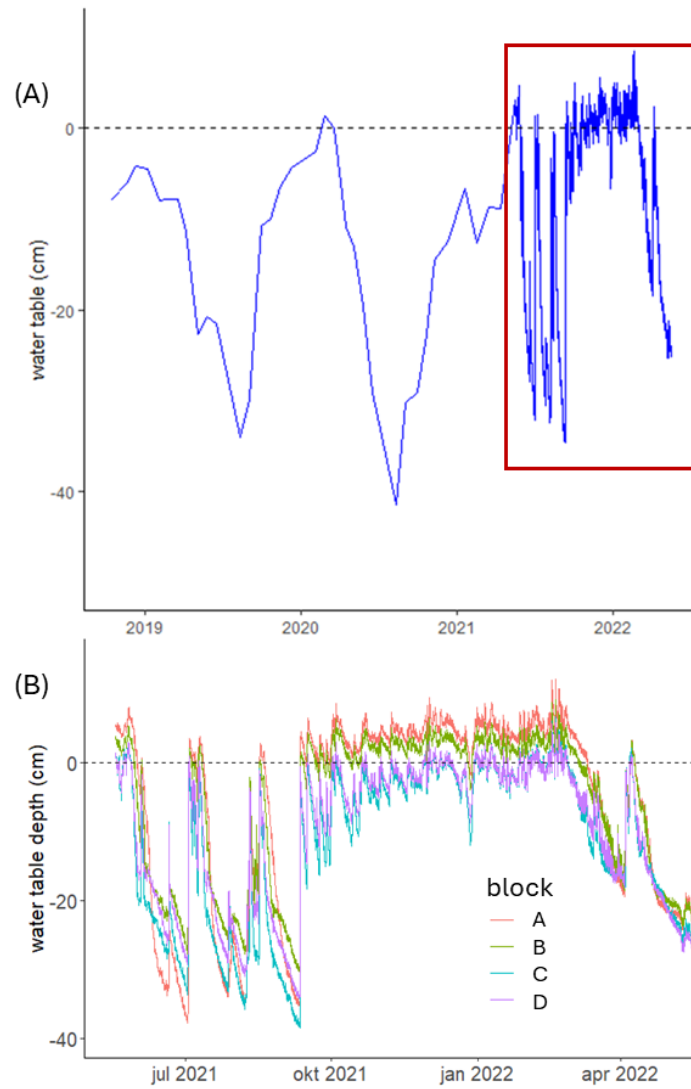
### 114 **2.1 Study area**

115 This study was conducted from May 2021 to May 2022 at a riparian fen peatland located in  
116 the Nørreå valley, Vejrumbro, Central Jutland, Denmark (56°26'15.3''N, 9°32'44.1''E) (Fig  
117 1). The site was drained in the 1930s and used for agriculture predominantly under grassland  
118 rotation and grazing. The field became gradually wetter because of land subsidence, and the  
119 water level was largely controlled by the Nørreå stream, located at the southern border of the

120 peatland (Malinowski et al., 2015). After 2018, maintenance of the drainage ditches stopped  
 121 and the mean annual WTD gradually increased during the following years reaching -8 cm  
 122 during the study year (18 May 2021 to 17 May 2022), with a minimum of -35 cm in the  
 123 summer and a maximum of 8 cm in the winter across the experimental blocks (Fig 2a). The  
 124 mean air temperature and total precipitation during the study year, measured at the  
 125 Foulumgard meteorological station (Danish Meteorological Institute), located 6 km from the  
 126 study site, were 9 °C and 709 mm, respectively. The peat layer at the study site has an  
 127 average depth of 2 m, covering up to 10 m of gyttja (Mashadi et al., 2024). The  
 128 physicochemical characteristics of the peat were measured for the top 1 meter of the soil as  
 129 part of a previous study (Table 1) by Nielsen et al. (2023b).



130  
 131 Figure 1. A, map of Denmark, red star indicates the study site location; B, aerial photograph  
 132 of study site, letters indicate the four studied blocks, and yellow star indicates where the ditch  
 133 water samples were taken from; C, diagram of one of the blocks showing the three  
 134 randomized harvest treatment plots (0-cut, 2-cut, and 5-cut) and the location of collars (red  
 135 squares) and piezometers (blue cylinders); D, transparent chamber with shroud used for gas  
 136 measurements.



137

138 Figure 2. Panel (A) presents WTD across the experimental blocks as measured in each block  
 139 with intervals of 2-3 weeks at the study site from October 2018 to April 2021 and every hour  
 140 from May 2021 until May 2022 (red square). Panel (B) presents the hourly WTD shown in the  
 141 red square as the mean of each block with different colors.

142 Table 1. Soil physicochemical characteristics across 0-100 cm depth in the four studied  
 143 blocks (A-D).

144

Plot	OM	pH	pb	TC	TN	C:N
	%		$\text{g cm}^{-3}$	$\text{g kg}^{-1}$	$\text{g kg}^{-1}$	
A	85	5.6	0.15	440	26	17
B	83	6.0	0.15	430	28	14
C	70	6.2	0.18	374	24	15
D	75	6.2	0.13	401	27	15
Mean	78	6.0	0.15	411	26	15

145 †OM, organic matter;  $\rho_b$ , bulk density; TC, total C; TN, total N; C:N, carbon to nitrogen  
146 ratio.

147

## 148 **2.2 Experimental design**

149 Four blocks (indicated by A, B, C and D on Fig 1B) were established with reed canary grass  
150 (RCG, *Phalaris arundinacea*, cultivar Lipaula) in 2018 as part of a larger field experiment.

151 Each block had six randomly placed plots with six different harvest and fertilization

152 treatments whereof only three (0-cut, 2-cut, 5-cut; referring to the number of harvest events

153 applied) were used for this study. Thus, the experimental design of this study consists of four

154 replicate blocks, each with three harvest/fertilization treatments. Harvest and fertilization

155 dates are shown in Figure 3. The harvested plots were fertilized with 200 kg N ha<sup>-1</sup> and 178

156 kg K ha<sup>-1</sup> in total, given as NPK 18-0-16 in equal split doses. Thus, the 2-cut and the 5-cut

157 received 100 kg N ha<sup>-1</sup> and 40 kg N ha<sup>-1</sup> for each cut, respectively, while the 0-cut did not

158 receive any fertilizer. The dimensions of the blocks and plots were (16 x 18 m), and (16 x 3

159 m), respectively (Fig 1C). Further details of the experimental design can be found in Nielsen

160 et al. (2021). At each plot, one 55 x 55 cm collar was installed to 10 cm depth to facilitate

161 closed, non-steady-state chamber measurements of net CO<sub>2</sub> and CH<sub>4</sub> fluxes. A piezometer

162 with a screen from 5 cm to 100 cm soil depth was installed 10-20 cm away from the collar for

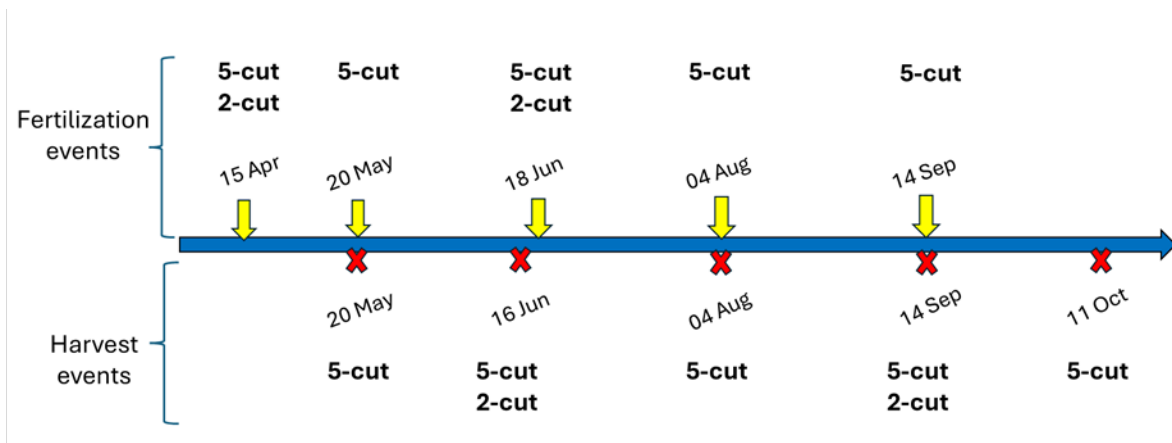
163 soil water sampling. Ts at 5 cm soil depth and WTD were measured continuously at hourly

164 intervals using Ts dataloggers (HOBO Pendant temperature/light 64K data logger; Onset

165 Corporation, Massachusetts, USA), and Leveloggers (Levelogger 5 Junior; Solinst Canada

166 Ltd, Ontario, Canada), respectively. Perforated gauge tubes for the leveloggers sealed with

167 lids and soil temperature loggers were installed in 2020 inside the collars.



168

169 Figure 3. Timeline of fertilization and harvest events applied to the 2-cut and 5-cut harvest  
170 treatments during 2021-22.

171

172 **2.3 Net carbon dioxide and methane flux measurements**

173 The CO<sub>2</sub> and CH<sub>4</sub> measurements were performed biweekly +/- one week between 10:00 am  
174 and 3:00 pm on days of predominantly clear sky conditions from 28 May 2021 to 14 June  
175 2022. A total of 26 campaign measurements were undertaken. Fluxes were measured using a  
176 fully transparent chamber (60 cm x 60 cm x 41 cm) made of Plexiglass and equipped inside  
177 with a photosynthetic active radiation (PAR) sensor (190-SA; Li-Cor Inc., Lincoln, NE,  
178 USA), a temperature sensor, and an air mixing fan. Further details of the chamber design and  
179 how the temperature was controlled during operation can be found in Elsgaard et al. (2012).  
180 The chamber was connected to an LGR-ICOS™ GLA131-GGA microportable gas analyzer  
181 (ABB Ltd.), which simultaneously measured water vapor corrected CO<sub>2</sub> and CH<sub>4</sub> (i.e., dry  
182 fractions) at 1 Hz resolution. Chamber deployment was 120 s per measurement. All data were  
183 stored using a Campbell CR1000X data logger (Campbell Sci. Logan, UT, USA) with the  
184 same timestamp. In order to fit the RCG inside the chamber during growth, a chamber  
185 extension with the same dimensions as the measurement chamber was used during all  
186 measuring campaigns, i.e. total chamber height with the extension was 82 cm. Measurements  
187 were conducted during constant PAR conditions, when possible, by timing measurements

188 such that changing cloud conditions were avoided. For each campaign and at each soil collar,  
189 fluxes were measured corresponding to four PAR levels by using net shrouds and an opaque  
190 cover as described by Kandel et al. (2017). This resulted in four flux measurements, one  
191 under fully transparent conditions which corresponded to net ecosystem exchange (NEE), a  
192 second under ca. 50% blocked PAR, a third under ca. 75% blocked PAR, and a fourth under  
193 100% blocked PAR equivalent to  $R_{eco}$ . Between PAR levels plants were given one minute to  
194 adapt to the new PAR conditions while the chamber was lifted on one side, allowing air  
195 circulation and bringing  $CO_2$  and  $CH_4$  concentrations to atmospheric levels.

196 All fluxes were calculated using the Flux package 0.3-0.1 (Jurasinski et al., 2022) in R (R  
197 Core Team (2023), R version 4.3.0). Inspection of fluxes revealed that fluxes were mostly  
198 linear, and flux rates were therefore calculated based on linear regression. For low  $CO_2$  fluxes  
199 ( $<100 \text{ mg } CO_2 \text{ m}^{-2} \text{ h}^{-1}$ ), fluxes with an  $R^2 < 0.6$  and a  $nrmse > 0.1$  were removed, while for  
200 high  $CO_2$  fluxes ( $>100 \text{ mg } CO_2 \text{ m}^{-2} \text{ h}^{-1}$ ), fluxes with an  $R^2 < 0.9$  and a  $nrmse > 0.1$  were  
201 identified and the PAR and  $CO_2$  flux were manually inspected. If sudden changes in the PAR  
202 occurred during the 2 min measurement period or if the flux curve indicated a possible  
203 leakage, flux data were discarded. These criteria resulted in 3% of the calculated  $CO_2$  fluxes  
204 being removed. In the case of  $CH_4$ , ebullitions were excluded by using the *fluxx* function of  
205 the Flux package, which automatically detects and excludes rapid concentration fluctuations  
206 while calculating fluxes. The resulting calculated linear  $CH_4$  fluxes had  $R^2$  values higher than  
207 0.9, therefore no fluxes were removed based on non-linearity. If a possible leakage was  
208 identified by negative or non-linear  $R_{eco}$  fluxes, fluxes were removed, resulting in 1.6% of the  
209 fluxes removed. For further calculations, only the  $CH_4$  fluxes measured under 100% PAR  
210 blocked (opaque conditions) were used.

## 211 **2.4 Biomass measurements**

212 Spectral reflectance was measured in all collars biweekly at gas sampling days and before  
213 and after harvest events using a portable crop sensor (RapidSCAN CS-45; Holland Scientific  
214 Inc., Lincoln, NE, USA), which was held 30 cm above the canopy and horizontally rotated  
215 45° while performing measurements to cover all vegetation inside the collar. Approximately  
216 30 scans were taken per collar and their mean values were used to calculate the ratio  
217 vegetation index (RVI) as the ratio between the near-infrared and the red light reflectance.  
218 The RVI has been used as a proxy for photosynthetically active biomass and it has been used  
219 in photosynthesis and ecosystem respiration models (Kandel et al., 2017; Karki et al., 2019).  
220 Hourly RVI values were obtained by linearly interpolating biweekly RVI measurements, and  
221 used in GPP and  $R_{\text{eco}}$  modelling. Fresh weight yield and dry matter content were determined  
222 by harvesting the biomass inside the collars at respective cuts and analyzed for total N and C  
223 with a Vario Max CN (Elementar Analysesysteme GmbH, Hanau, Germany). Dry matter  
224 yields (Table A1) were multiplied by percentage C to obtain the yield in  $\text{C ha}^{-1} \text{ yr}^{-1}$  as part of  
225 the  $\text{CO}_2$ -C budget. The sum of yields from individual cuts per treatment was considered as  
226 the annual yield.

## 227 **2.5 Gap filling models and annual budgets**

228 The measured NEE  $\text{CO}_2$  fluxes were partitioned into GPP and  $R_{\text{eco}}$ . The GPP was calculated  
229 for all PAR levels as  $\text{NEE} - R_{\text{eco}}$ . From an atmospheric perspective we always consider  $R_{\text{eco}}$   
230 positive, and GPP negative while NEE can be either positive (ecosystem carbon source) or  
231 negative (ecosystem carbon sink). The net ecosystem carbon balance of  $\text{CO}_2$  (NECB) was  
232 calculated as the sum of the NEE plus the harvested yields for the 2-cut and 5-cut treatments.  
233 For calculation of annual budgets, three models from previous studies (one for GPP and two  
234 for  $R_{\text{eco}}$ , see below) were used. Additionally, a fourth model was developed based on a

235 modification of the two selected  $R_{eco}$  models. The GPP was modelled based on Karki et al.  
 236 (2019) (model 1).

$$237 \quad GPP = \frac{GPP_{max} * PAR}{k + PAR} * \left( \frac{RVI}{RVI + \alpha} \right) * FT \quad (\text{model 1})$$

238 where GPP is in  $mg \text{ CO}_2 \text{ m}^{-2} \text{ h}^{-1}$ ,  $RVI$  is the ratio vegetation index,  $k$  is the PAR value at  
 239 which GPP reaches 50%,  $\alpha$  is a fitted parameter, and  $FT$  is a linear temperature dependent  
 240 function set to 0 when temperature  $< -2 \text{ }^\circ\text{C}$  and to 1 when temperature  $> 10 \text{ }^\circ\text{C}$  (Kandel et al.  
 241 2017).

242  $R_{eco}$  was modelled based on Karki et al. (2019) with RVI and  $T_s$  as input variables (model 2),  
 243 based on Rigney et al. (2018) with WTD and  $T_s$  as input variables (model 3), and with a new  
 244 model, which included RVI, WTD and  $T_s$  as input variables (model 4).

$$245 \quad Reco = t1 + (a * RVI) * e^{\left[ b * \left( \frac{1}{T_{10} - T_0} - \frac{1}{T_s - T_0} \right) \right]} \quad (\text{model 2})$$

$$246 \quad Reco = t1 * e^{\left[ b * \left( \frac{1}{T_{10} - T_0} - \frac{1}{T_s - T_0} \right) \right]} + (WTD + c)^2 \quad (\text{model 3})$$

$$247 \quad Reco = t1 + (a * RVI) + [(WTD - WTD_{max}) * c]^2 * e^{\left[ b * \left( \frac{1}{T_{10} - T_0} - \frac{1}{T_s - T_0} \right) \right]} \quad (\text{model 4})$$

248 where  $R_{eco}$  is in  $mg \text{ CO}_2 \text{ m}^{-2} \text{ h}^{-1}$ ,  $RVI$  is the ratio vegetation index,  $WTD$  is the water table  
 249 depth (cm),  $WTD_{max}$  is the maximum WTD (cm),  $t1$ ,  $a$ ,  $b$ , and  $c$  are fitted parameters,  $t1$  has a  
 250 lower limit set at 1, while all other fitted parameters are without upper and lower limits.  $T_{10}$  is  
 251 the reference temperature set to  $10 \text{ }^\circ\text{C}$ ,  $T_0$  is the zero-respiration temperature set to  $-46 \text{ }^\circ\text{C}$ ,  
 252 and  $T_s$  is the soil temperature ( $^\circ\text{C}$ ) at 5 cm depth.

253

254 Each  $R_{eco}$  model was fitted to data obtained biweekly using non-linear regression (non-least  
 255 square) in R (R Core Team (2023), R version 4.3.0) for each plot independently. Annual  $\text{CO}_2$   
 256 budgets were calculated using the parameterized models, hourly  $T_s$ , WTD, and RVI. Model  
 257 performance was evaluated by comparing the measured GPP and  $R_{eco}$  with the modelled  
 258 values using the following indices: Nash-Sutcliffe efficiency, which indicates how well the  
 259 plot of observed versus simulated data fits the 1:1 line, with more accurate models having  
 260 values closer to 1, corrected Akaike information criterion (AICc), normalized root mean  
 261 square error, and  $R^2$  using the hydroGOF package in R (Zambrano-Bigiarini, 2020). Based on

262 these criteria, the best performing  $R_{\text{eco}}$  model was used to calculate the annual  $\text{CO}_2$  budget. In  
263 addition, field models of  $R_{\text{eco}}$  (model 4) and GPP were parameterized by pooling data from all  
264 blocks and treatment plots. For  $\text{CH}_4$ , measured fluxes were linearly interpolated to obtain the  
265 annual  $\text{CH}_4$  budget.

266 We tested the sensitivity of the best performing  $R_{\text{eco}}$  model (model 4) to the frequency of  
267 WTD data either using (a) hourly WTD, Ts, and RVI (b) annual mean WTD with hourly Ts  
268 and RVI, and (c) annual mean WTD, annual mean Ts, and hourly RVI.

## 269 **2.6 Water chemistry**

270 Soil pore water was collected biweekly at the same time as the gas campaigns and analyzed  
271 for total organic C (TOC), dissolved organic C (DOC), total nitrogen (TN), total dissolved  
272 nitrogen (TDN), nitrate-N, ( $\text{NO}_3$ ), ammonia-N ( $\text{NH}_4$ ), total P (TP), total dissolved P (TDP),  
273 Fe, pH, electroconductivity (EC), and turbidity. Pore-water samples were collected  
274 immediately after each GHG measurement from the piezometers installed 20 cm from each  
275 GHG collar. Water samples were extracted with a syringe from a tube with the other end  
276 attached to an aquarium air stone (Air Stone Economy Cylinder 4 X 5 cm, Aquakoi / JV  
277 Trading Aps) placed 20 cm below the water table in each piezometer. An additional sample  
278 was collected from a ditch draining the peatland. A total of 13 samples were collected per  
279 campaign for a total of 338 samples. Upon collection, part of the sample was filtered using  
280  $0.45 \mu\text{m}$  pore size filter. The unfiltered samples were analyzed for pH and electroconductivity  
281 (EC) following the Danish Standards DS287 and DS288, respectively, turbidity, TN  
282 following Best (1976), TP using the Danish Standard, DS291 photometric method (Dansk  
283 Standard, 2004), TOC using a total organic C analyzer (TOC-VCPH; Shimatzu Corporation,  
284 Kyoto, Japan), and Fe by ICP emission spectrometer (iCAP 6000 series; Thermo Fisher  
285 Scientific, Inc., Walthman, Massachusetts, USA). The filtered samples were analysed for

286 DOC with a (TOC-VCPH; Shimatzu Corpotation, Kyoto, Japan), TDN and NO<sub>3</sub> (Best, 1976),  
287 TDP by the Danish Standard, DS291 photometric method (Dansk Standard, 2004), and NH<sub>4</sub>  
288 following Crooke and Simpson (1971).

## 289 **2.7 Statistical analysis**

290 Statistics were performed in R (R Core Team (2023), R version 4.3.0). Effects were  
291 considered significant if *p value* < 0.05. Normality assumptions were evaluated with Q-Q  
292 plots, histograms, and residual plots. Kruskal-Wallis tests were used to test the effect of  
293 harvest treatment and block on R<sub>eco</sub>, GPP, NEE, and NECB. Correlations and principal  
294 component analysis (PCA) were used to establish relationships between water chemistry  
295 parameters, R<sub>eco</sub>, GPP, NEE, Ts, RVI, PAR, WTD, and CH<sub>4</sub>.

296 ANOVA and Tukey tests were used to determine differences between water chemistry  
297 parameters among blocks and harvest treatments. The effects of each water chemistry  
298 parameter on R<sub>eco</sub> and GPP were tested with linear mixed models. Each water chemistry  
299 parameter was added one by one as a fixed factor to the base models shown below as models  
300 5 and 6, and the performance of the model including each water chemistry parameter was  
301 compared to the base model. The R<sub>eco</sub> base model included WTD, Ts, and RVI as fixed  
302 factors and the measuring campaign and replicate block as random factor (model 5), while  
303 the GPP base model included PAR, Ts, and RVI as fixed factors and measuring campaign and  
304 replicate block as random factors (model 6).

305  $Reco = Harvest\ treatment + WTD + Ts + RVI + (campaign) + (R.Plot)$  (model 5)

306  $GPP = Harvest\ treatment + PAR + Ts + RVI + (campaign) + (R.Plot)$  (model 6)

307 Likelihood ratio tests were used to assess if the base models were significantly improved by  
308 adding a water chemistry parameter. If this was the case, the R<sup>2</sup> and root mean square error

309 (RMSE) were calculated. Outliers of the water chemistry data were identified as being larger  
310 than 3 times the standard deviation for each parameter independently excluding 1% of the  
311 data from the analyses.

### 312 **3. Results**

#### 313 **3.1 Carbon balance**

314 Management had a marginally significant effect on GPP (Kruskal-wallis test; p value < 0.1;  
315 n: 12), with more negative GPP (larger CO<sub>2</sub> uptake) in the five-cut treatment ( $-20.2 \pm 0.7$  t  
316 CO<sub>2</sub>-C ha<sup>-1</sup> yr<sup>-1</sup>; mean ± SE) and lowest in the 0-cut treatment ( $-15.5 \pm 1.3$  t CO<sub>2</sub>-C ha<sup>-1</sup> yr<sup>-1</sup>)  
317 (Table 2). No significant effects of management on R<sub>eco</sub> (between  $22.1 \pm 2.5$  and  $22.4 \pm 3.3$  t  
318 CO<sub>2</sub>-C ha<sup>-1</sup> yr<sup>-1</sup>; p value = 0.98) and NEE (between  $2.2 \pm 0.5$  and  $6.9 \pm 2.2$  t CO<sub>2</sub>-C ha<sup>-1</sup> yr<sup>-1</sup>;  
319 p value = 0.22) were registered although the NEE of 0-cut was 4.6 t CO<sub>2</sub>-C ha<sup>-1</sup> yr<sup>-1</sup> higher  
320 than the two managed treatments on average. The 2-cut and 5-cut treatments gave similar  
321 annual biomass yields ( $4 \pm 0.7$  and  $4 \pm 0.2$  t C ha<sup>-1</sup> yr<sup>-1</sup>, respectively) leading to similar  
322 NECB for all treatments when the exported yields were added to the NEE (between  $6.0 \pm 0.5$   
323 and  $6.9 \pm 2.2$  t CO<sub>2</sub>-C ha<sup>-1</sup> yr<sup>-1</sup>). Biomass yields of the 2-cut treatment were similar for both  
324 harvesting events, but much lower in block A compared to the other blocks, while for the 5-  
325 cut treatment yields peaked at the third harvest and were lowest at the fifth. There were less  
326 yield differences between blocks for the 5-cut treatment compared to the 2-cut treatment.  
327 Block D had the highest yields of both 2-cut and 5-cut treatments.

328 Although the experimental site looked rather uniform, large differences were seen between  
329 blocks, especially for Reco and NEE, the latter with coefficients of variation of 0.56, 0.71,  
330 and 0.41, for the 0-cut, 2-cut, and 5-cut, respectively. The lowest R<sub>eco</sub> was registered in block  
331 A, followed by block B, and the highest R<sub>eco</sub> was in blocks C and D (p<0.05) (Table 2, Fig 4).  
332 Differences in GPP between blocks were not significant despite lower CO<sub>2</sub> uptake leading to

333 lower biomass production in block A. No significant difference in NEE was observed  
334 between blocks because the higher  $R_{\text{eco}}$  was accompanied by larger  $\text{CO}_2$  uptake (more  
335 negative GPP) and thus higher biomass production. Figure 5 shows that the cumulative NEE  
336 grew faster in blocks C and D than in blocks A and B leading to approximately eight times  
337 higher annual NEE in blocks C and D compared to block A for the 0-cut treatment. The  
338 NECB was marginally different ( $p$  value  $< 0.1$ ) between blocks, with lowest NECB in block  
339 A, followed by block B, and highest in block C and D indicating that within field  
340 heterogeneity overrides treatments. However, the interaction between treatment and block  
341 indicated that harvest of biomass considerably reduced net  $\text{CO}_2$  emission in the more  
342 productive blocks (C and D) while little effect on NEE was seen for the less productive  
343 blocks (A and B) (Figure 5).

344 Cumulated methane emissions averaged  $113 \text{ kg CH}_4 \text{ ha}^{-1} \text{ yr}^{-1}$  for the studied year and varied  
345 primarily by block with less emissions at block C and largest emissions at block A (Table 3  
346 and Fig. A3). Methane had no significant correlations with nutrients (Fig. A1), except  $\text{NH}_4$ ,  
347 which had a negative correlation with  $\text{CH}_4$ .  $\text{CH}_4$  also had a positive correlation with  $R_{\text{eco}}$  and  
348 Ts but no significant correlation with WTD.

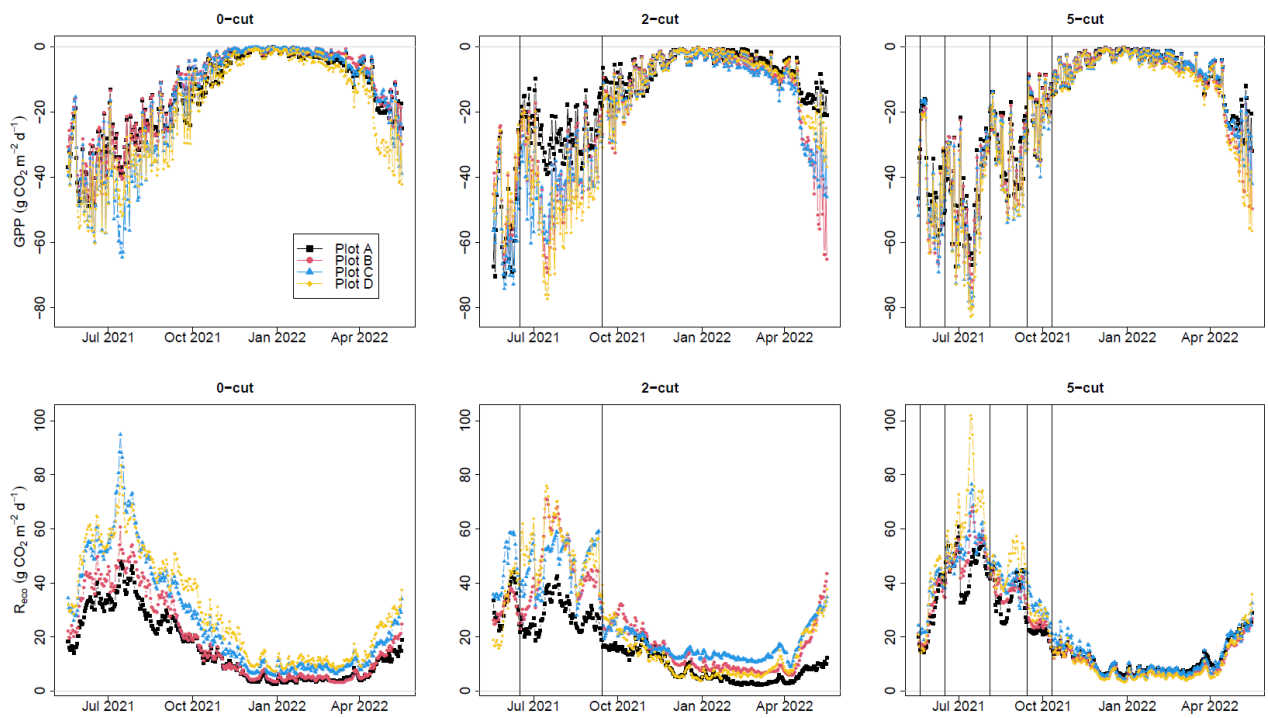
349 Table 2. Cumulated CO<sub>2</sub>-C emission for the four studied blocks and harvest treatments during  
 350 the study year.

Block	Treatment	R <sub>eco</sub>	GPP	NEE	Yield	NECB
		t CO <sub>2</sub> -C ha <sup>-1</sup> yr <sup>-1</sup>	t CO <sub>2</sub> -C ha <sup>-1</sup> yr <sup>-1</sup>	t CO <sub>2</sub> -C ha <sup>-1</sup> yr <sup>-1</sup>	t C ha <sup>-1</sup> yr <sup>-1</sup>	t C ha <sup>-1</sup> yr <sup>-1</sup>
A	0-cut	15.4	-14.2	1.2	NA	1.2
B		18.6	-13.0	5.6	NA	5.6
C		26.2	-16.0	10.2	NA	10.2
D		29.4	-18.9	10.6	NA	10.6
Mean ± SE		22.4 ± 3.3	-15.5 ± 1.3	6.9 ± 2.2	NA	6.9 ± 2.2
A	2-cut	14.9	-15.3	-0.4	1.9	1.5
B		23.6	-20.8	2.8	4.5	7.3
C		26.4	-22.0	4.3	4.6	9.0
D		23.7	-20.6	3.1	5.0	8.1
Mean ± SE		22.1 ± 2.5	-19.7 ± 1.5	2.5 ± 1	4.0 ± 0.7	6.5 ± 1.7
A	5-cut	20.6	-18.5	2.2	3.5	5.6
B		21.0	-20.2	0.8	3.9	4.7
C		23.7	-20.4	3.3	3.5	6.8
D		24.3	-21.9	2.4	4.5	6.9
Mean ± SE		22.4 ± 0.9	-20.2 ± 0.7	2.2 ± 0.5	3.8 ± 0.2	6.0 ± 0.5

351

352 R<sub>eco</sub> is ecosystem respiration, GPP is gross primary productivity, NEE is net ecosystem  
 353 exchange, and NECB of CO<sub>2</sub> is net ecosystem carbon balance (NEE + yield).

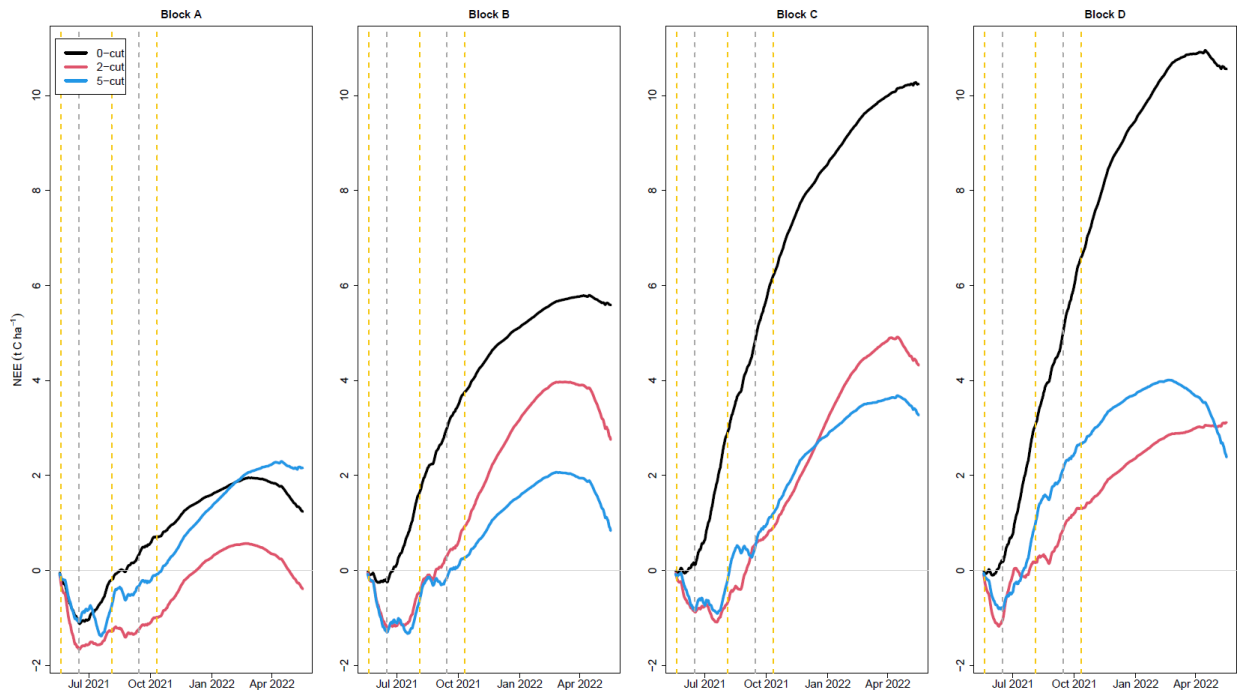
354



355

356 Figure 4. Modelled daily gross primary productivity (GPP) (top) and ecosystem respiration  
357 ( $R_{eco}$ ) (bottom) for the three management treatments (0-cut, 2-cut, and 5-cut). Colors indicate  
358 the four block replicates. Vertical lines are harvesting events.

359



360

361 Figure 5. Cumulative net ecosystem exchange for the four studied blocks and three harvest  
 362 treatments. Black line is the 0-cut, red line is the 2-cut, and blue line is the 5-cut.  
 363 Vertical gray dashed lines are harvest events for only the 2-cut treatment while all vertical  
 364 dashed lines are harvest events for both the 2-cut and 5-cut treatments.

365 Table 3. Cumulated methane emissions for the blocks (A, B, C, D) and harvest treatments 0-  
 366 cut, 2-cut, and 5-cut during the study year.

Block	Treatment	CH <sub>4</sub> emissions kg CH <sub>4</sub> ha <sup>-1</sup>
A	0-cut	200.2
	2-cut	157.5
	5-cut	125.7
	mean ± SD	161.1 ± 30.5
B	0-cut	124.0
	2-cut	129.0
	5-cut	99.4
	mean ± SD	117.5 ± 12.9
C	0-cut	35.7
	2-cut	40.1
	5-cut	73.7
	mean ± SD	49.8 ± 17
D	0-cut	114.5
	2-cut	190.0
	5-cut	67.6
	mean ± SD	124.0 ± 50.4
Total mean		113.1

367

### 368 **3.2 Model performance**

369 Measured  $R_{\text{eco}}$  was best described by model 4 in 11 out of the 12 studied plots based on the  
370 NSE and in 10 out of 12, based on the AICc (table 4). The other calculated indices ( $R^2$ , and  
371 NRMSE) also supported model 4 as the best overall performing model. Additional 1:1 plots  
372 of measured vs. modelled  $R_{\text{eco}}$  for model 4 can be seen in Figure A2 in appendix. When WTD  
373 was excluded as seen in model 2 compared to model 4, the overall performance was reduced  
374 as indicated by lower NSE for most plots except for plot C 5-cut and plot D 0-cut (Table 4).  
375 Model 3, where RVI was excluded, had the lowest performance of the three tested models. In  
376 general, the 0-cut plots provided the best model performances (highest NSE),  $R^2 > 0.9$ , and  
377 the lowest AICc, while the 2-cut and 5-cut plots had lower model performances (between  
378 0.74 and 0.92 NSE). The performance results for the GPP models had  $R^2$  values that ranged  
379 between 0.81 and 0.96 (Table A3).

380  $R_{\text{eco}}$  was positively correlated with  $T_s$  and RVI, and negatively correlated with WTD (lower  
381 WTD = deeper water table). On the other hand, GPP was negatively correlated to  $T_s$ , RVI,  
382 and PAR, meaning that larger  $T_s$ , RVI, and PAR correlate to larger  $\text{CO}_2$  uptake. These  
383 expected relationships seen in the PCA plots (Fig 6) and correlations statistics (Fig. A1)  
384 support why the variables in models 1-4 were selected and parameterized in this study. The  
385 fitted parameter values of the best performing  $R_{\text{eco}}$  model and the GPP model varied between  
386 plots (Fig 7). For the  $R_{\text{eco}}$  model, the  $b$  parameter was near its maximum value in most plots,  
387 while for the GPP model, the  $k$  parameter was near its maximum in most plots.

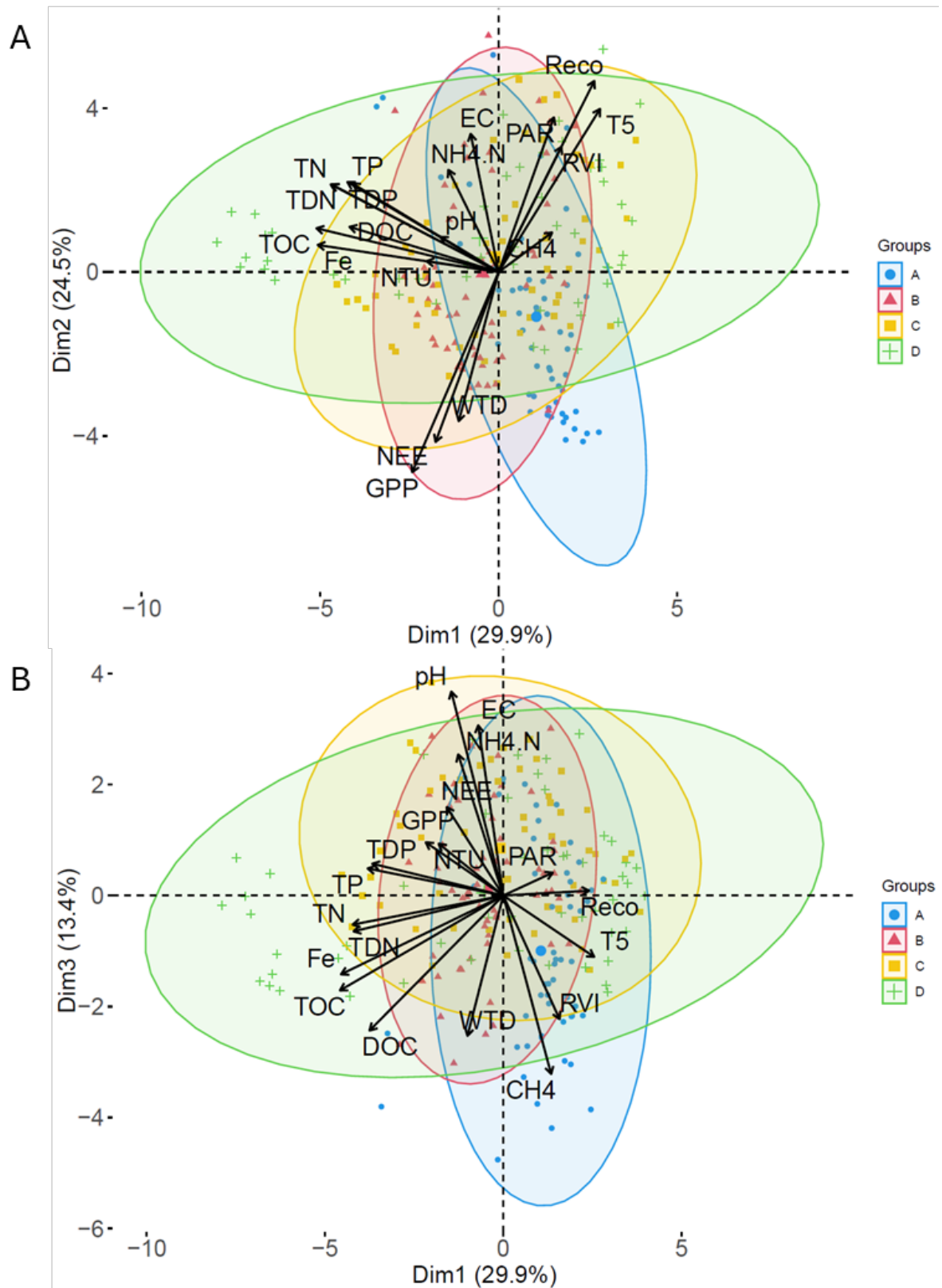
388 Table 4. Evaluation of three  $R_{eco}$  models parameterized for each plot by four different  
 389 performance indices.

390

Block	Treatment	Model 2				Model 3				Model 4			
		R2	NRMSE	NSE	AICc	R2	NRMSE	NSE	AICc	R2	NRMSE	NSE	AICc
A	0	0.95	21.4	0.95	980	0.96	19.4	0.96	1216	0.97	16.7	0.97	943
	2	0.85	39.2	0.84	1090	0.7	54.7	0.7	1424	0.88	34.8	0.88	1073
	5	0.71	53.5	0.71	1247	0.84	39.9	0.84	1481	0.82	42.5	0.82	1211
B	0	0.95	21.6	0.95	1029	0.93	26	0.93	1331	0.98	15.4	0.98	978
	2	0.71	53.3	0.71	1261	0.67	57.4	0.67	1570	0.74	50.7	0.74	1255
	5	0.83	40.7	0.83	1113	0.85	39	0.85	1389	0.85	38.3	0.85	1106
C	0	0.96	19.3	0.96	1109	0.92	27.7	0.92	1446	0.96	18.7	0.96	1106
	2	0.77	47.8	0.77	1175	0.71	53.8	0.71	1565	0.81	43.9	0.8	1163
	5	0.84	39.6	0.84	1227	0.84	39.9	0.84	1519	0.84	39.6	0.84	1229
D	0	0.9	32.1	0.9	1030	0.87	36.4	0.87	1348	0.9	32.1	0.9	1032
	2	0.82	41.8	0.82	1229	0.81	43.3	0.81	1533	0.88	34.3	0.88	1198
	5	0.91	31.1	0.9	1153	0.84	40.1	0.84	1484	0.92	28.5	0.92	1142

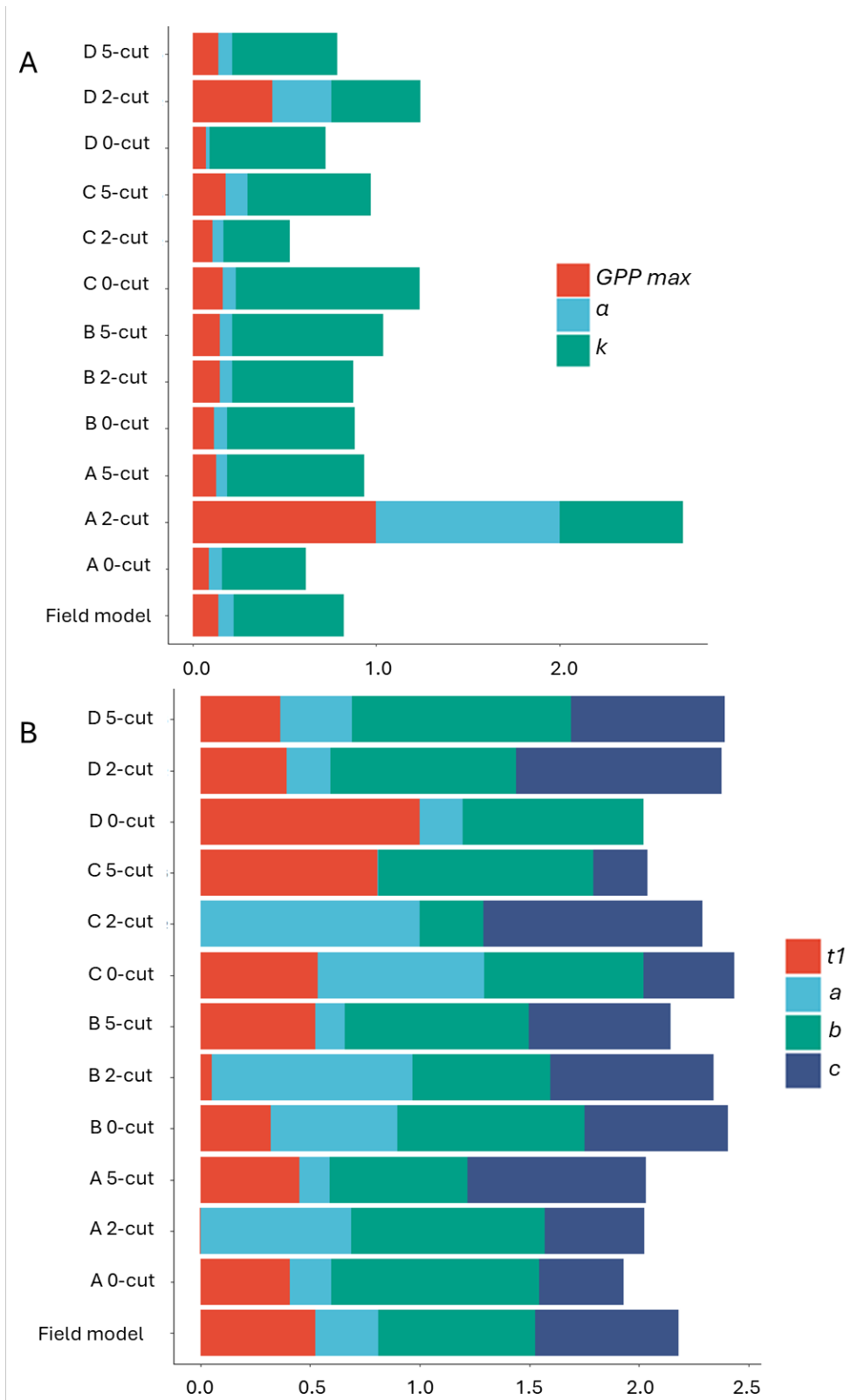
391 A, B, C, and D are the four blocks, The three harvest treatments at each block (plots) are 0, 2,  
 392 and 5. The four indexes of model evaluation are:  $R^2$ , normalized root mean square of error  
 393 (NRMSE), Nash-Sutcliffe efficiency (NSE), and corrected Akaike information criterion  
 394 (AICc).

395



396

397 Figure 6. Principal component analysis plots. PC1 vs PC2 (A), PC1 vs PC3 (B). Variability  
 398 explained by each PCA is the value in parenthesis. Colors represent the four studied blocks.  
 399 Harvest treatments are combined.



400

401 Figure 7. Variability of parameters fitted in  $R_{eco}$  model 4 (A) and the GPP model (B). Each bar  
 402 represents a plot, and the bottom bar corresponds to the field model. Each color represents a  
 403 different parameter. Parameter values were normalized i.e. dividing them by the maximum  
 404 value.

405

406

409

### 410 3.3 Sensitivity analysis using WTD with different temporal resolution

411 Using annual mean WTD and Ts as input for model 4 instead of hourly values,

412 underestimated  $R_{eco}$  between 9 to 26% for all plots with an average of 18% (Fig 8) (Table

413 A4). On the other hand, using the annual mean WTD along with hourly Ts generally followed

414 similar trends in  $R_{eco}$  as using hourly input data, but high emission events were slightly

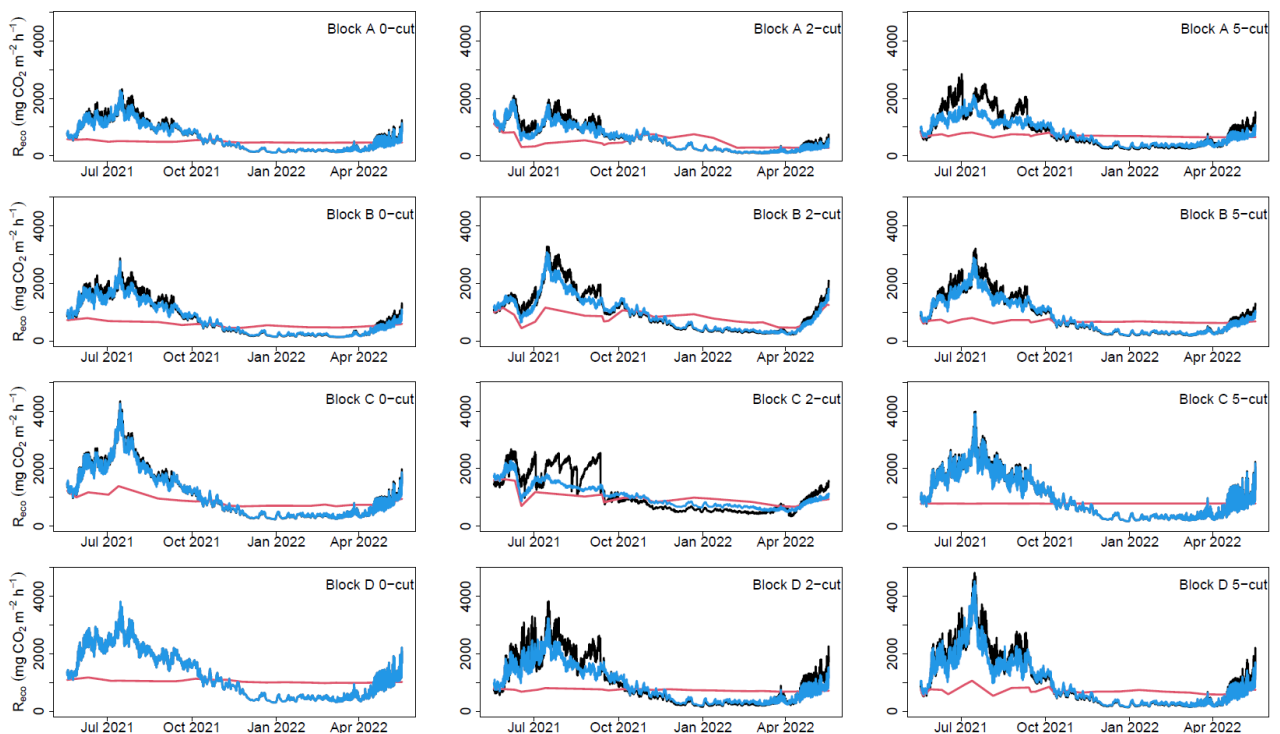
415 underestimated resulting in an underestimation that ranged between 0 and 10% with an

416 average of 5% for all plots when compared to the model that used hourly data (Fig 8) (Table

417 A4). If the  $R_{eco}$  was calculated using annual mean WTD and annual mean Ts, or annual mean

418 WTD along with hourly Ts, the  $CO_2$  budget resulted in a total mean NECB of 2.6 and 5.3 t C

419  $ha^{-1} yr^{-1}$ , respectively.



420

421 Figure 8. Sensitivity of ecosystem respiration ( $R_{eco}$ ) modelled for all plots to the data  
422 frequency of water table depth (WTD). Black lines represent  $R_{eco}$  modelled with hourly  
423 WTD, soil temperature (Ts), and RVI, blue line represents  $R_{eco}$  modelled with mean annual  
424 WTD, hourly Ts, and hourly RVI, and red line represents  $R_{eco}$  modelled with mean annual  
425 WTD, mean annual Ts, and hourly RVI.

### 426 3.4 Water chemistry

427 The PCA described in total 67.8 % of the variance in data by the first three principal  
428 components. PC1 and PC2 explained 29.9 and 24.7% of the variability in the data,  
429 respectively, while PC3 explained 13.4% of the variability (Fig 6). The PC1 VS PC2 plot  
430 shows clustering of the data with block D and A having the largest difference. PC1 describes  
431 the pore water nutrients, which are positively correlated with each other, and significance of  
432 correlations are presented in Figure A1. This shows that WTD had positive correlations with  
433 Fe, TOC and DOC and negative correlations with NH<sub>4</sub> and TDP, while Ts had negative  
434 correlations with all nutrients except NH<sub>4</sub> and TDP. Predominant correlations of nutrients  
435 with R<sub>eco</sub> were negative and positive with GPP and NEE, respectively.

436 Comparisons of water chemistry parameters between blocks indicated significant differences  
437 depending on type of nutrients. Generally, block (A) had the lowest nutrient concentrations,  
438 while block (D) had the highest nutrient concentrations, with the exception of DOC. The  
439 nutrient concentrations at the ditch appeared lower than the concentrations in the soil pore  
440 water at the blocks except for the TP and TDP (Table 5). Comparisons between harvest  
441 treatments showed that the 2 and 5-cut treatments had higher N and Fe concentrations than  
442 the 0-cut treatment, while there were no differences in other nutrients (Table 5). Additionally,  
443 the interaction between harvest treatment and block was significant for NH<sub>4</sub>,  
444 electroconductivity, pH, and turbidity.

445 The linear mixed model (Model 5) indicated that all nutrient concentrations, except NH<sub>4</sub>,  
446 significantly improved the base R<sub>eco</sub> model (Table 6), however the effect of TP, TDP, and pH  
447 also varied at plot level. For GPP, the addition of nutrients did not improve the base models,  
448 however pH and EC improved model 6 with its effect varying at plot level. The magnitude of  
449 model improvement (higher R<sup>2</sup> and lower RMSE) was larger for R<sub>eco</sub> than for GPP, however,

450 in general the R<sup>2</sup> and RMSE did not change considerably for all nutrients/parameters  
 451 compared to the base models (Table A5).

452 Table 5. Mean annual concentrations of water chemistry parameters at block A, B, C, and D,  
 453 and treatments 0-cut, 2-cut, and 5-cut.

Block	pH	EC	Turbidity	TOC	DOC	TN	TDN	NH <sub>4</sub> -N	NO <sub>3</sub> -N	TP	TDP	Fe
		mS cm <sup>-1</sup>	NTU	mg L <sup>-1</sup>	mg L <sup>-1</sup>	mg L <sup>-1</sup>	mg L <sup>-1</sup>	mg L <sup>-1</sup>	mg L <sup>-1</sup>	mg L <sup>-1</sup>	mg L <sup>-1</sup>	mg L <sup>-1</sup>
A	5.61 ± 0.05 (a)	0.19 ± 0.01 (a)	25.4 ± 2.01 (ab)	164 ± 9 (a)	129 ± 7 (a)	14.1 ± 0.9 (a)	12.8 ± 0.8 (a)	1.56 ± 0.25 (a)	4.98 ± 3.18	0.49 ± 0.04 (a)	0.40 ± 0.04 (a)	12.2 ± 0.9 (a)
B	6.40 ± 0.04 (c)	0.34 ± 0.01 (c)	29.6 ± 2.95 (b)	212 ± 7 (b)	160 ± 5 (b)	16.8 ± 0.4 (b)	15.5 ± 0.5 (b)	1.50 ± 0.15 (a)	1.38 ± 0.58	0.81 ± 0.04 (c)	0.69 ± 0.05 (b)	22.9 ± 1.1 (b)
C	6.22 ± 0.04 (b)	0.34 ± 0.01 (b)	40.3 ± 3.76 (c)	193 ± 10 (b)	135 ± 6 (ab)	18.6 ± 0.9 (b)	16.2 ± 0.7 (b)	3.34 ± 0.29 (b)	2.97 ± 1.49	0.68 ± 0.04 (b)	0.50 ± 0.03 (a)	19.0 ± 1.6 (b)
D	6.25 ± 0.04 (b)	0.32 ± 0.01 (b)	26.7 ± 3.85 (a)	209 ± 16 (b)	137 ± 8 (a)	19.6 ± 1.2 (b)	18.9 ± 1.2 (b)	2.95 ± 0.24 (b)	3.58 ± 1.90	1.07 ± 0.08 (c)	0.91 ± 0.08 (b)	36.3 ± 3.6 (c)
ditch	6.65 ± 0.07	0.32 ± 0.01	41.9 ± 32.9	66 ± 8	42 ± 3	7.2 ± 1.8	4.6 ± 0.3	1.2 ± 0.2	1.09 ± 0.21	1.13 ± 0.23	0.93 ± 0.2	3.9 ± 1.1
<b>Treatment</b>												
0	6.13 ± 0.05 (b)	0.26 ± 0.01 (a)	27.3 ± 2.4	191 ± 9	137 ± 5	16.0 ± 0.8 (a)	14.5 ± 0.7 (a)	1.96 ± 0.16 (a)	0.15 ± 0.03	0.83 ± 0.06	0.63 ± 0.05	20.3 ± 1.9 (a)
2	6.04 ± 0.05 (a)	0.31 ± 0.01 (b)	33.3 ± 3.0	189 ± 10	136 ± 6	18.5 ± 0.9 (b)	16.9 ± 0.9 (b)	2.69 ± 0.30 (b)	7.49 ± 2.64	0.71 ± 0.04	0.59 ± 0.05	23.3 ± 1.9 (b)
5	6.20 ± 0.04 (b)	0.33 ± 0.01 (c)	30.5 ± 3.1	203 ± 10	148 ± 6	17.3 ± 0.7 (ab)	16.1 ± 0.7 (ab)	2.36 ± 0.18 (ab)	1.87 ± 0.49	0.76 ± 0.05	0.63 ± 0.05	24.3 ± 2.2 (ab)

454

455 Total organic carbon (TOC), dissolved organic carbon (DOC), total nitrogen (TN), total  
 456 dissolved nitrogen (TDN), ammonia (NH<sub>4</sub>-N), nitrate (NO<sub>3</sub>-N), total phosphorus (TP), total  
 457 dissolved phosphorus (TDP), electrical conductivity (EC). Values are means ± standard error.  
 458 N values are 78, 25, and 104 for the blocks, ditch, and treatments, respectively. Letters in  
 459 parenthesis indicate significant differences between block (top) and harvest treatments  
 460 (bottom). The ditch was not included in statistical comparisons. No comparisons were  
 461 performed for NO<sub>3</sub> due to insufficient data.

462

463 Table 6. Effect of soil pore water chemistry parameters on ecosystem respiration (R<sub>eco</sub>, model  
 464 5) and gross primary productivity (GPP, model 6).

W.C. Parameter	R <sub>eco</sub> effect	GPP effect
TOC	Sig	Ns
DOC	Sig	Ns
TN	Sig	Ns
TDN	Sig	Ns
NH <sub>4</sub>	Ns	Ns
TP	Sig*	Ns
TDP	Sig*	Ns
Fe	Sig*	Ns
pH	Sig*	Sig*
Turbidity	Ns	Ns

465

466 Sig indicates significant improvement of the models by individually adding water chemistry  
 467 parameters. Sig\* indicates a significant effect that varied between harvest treatments. Ns  
 468 indicates not significant improvement. Water chemistry parameters included total organic  
 469 carbon (TOC), dissolved organic carbon (DOC), total nitrogen (TN), total dissolved nitrogen  
 470 (TDN), total phosphorus (TP), total dissolved phosphorus (TDP), and electrical conductivity  
 471 (EC). N = 312 for all water chemistry parameters.

472

473 **4. Discussion**

474 **4.1 Carbon balance**

475 **4.1.1 Annual budgets**

476 Comparison of results from this study to previous flux measurements on managed Danish  
 477 peatlands presented by Koch et al. (2023) shows that the total mean CO<sub>2</sub>-C emissions  
 478 (NECB) from this study ( $6.5 \pm 2.9 \text{ t C ha}^{-1} \text{ yr}^{-1}$ ; mean  $\pm$  SD) are larger than emissions from  
 479 other Danish organic soils under fertilization and similar WTD (between 0 and  $2.5 \text{ t C ha}^{-1} \text{ yr}^{-1}$   
 480 <sup>1</sup>; Koch et al., 2023). Similarly, our NECB is larger than emissions from peatlands at similar  
 481 WTD from both Germany (between  $-1.0 \text{ t C ha}^{-1} \text{ yr}^{-1}$  and  $1.5 \text{ t C ha}^{-1} \text{ yr}^{-1}$ ; Tiemeyer et al.,  
 482 2020) and the UK (between  $-2.0 \text{ t C ha}^{-1} \text{ yr}^{-1}$  and  $0.8 \text{ t C ha}^{-1} \text{ yr}^{-1}$ ; Evans et al., 2021). Our  
 483 NECB results are closer to the lower range of emissions from drained agricultural peatland  
 484 presented by Koch et al. (2023). Nielsen et al. (2024) reported the effect of management on  
 485 GHG emissions from 2020 to 2021 at the same study site as reported here, and found a higher  
 486 mean NECB of  $9.4 \text{ t C ha}^{-1} \text{ yr}^{-1}$  at the slightly lower mean annual WTD of -10 cm. Although  
 487 mean annual WTD increased only 2 cm, blocking of the drainage ditches resulted in  
 488 considerably higher WTD during summer 2021 envisaged by temporary flooded conditions.  
 489 Higher WTD along with a reduction of WTD fluctuations as rewetting progresses (Karimi et al.,  
 490 2024), could explain the lower NECB in 2021-22 compared to 2020-21 (Fig 2A). Other  
 491 studies have also shown a delay in reaching carbon neutral conditions despite drainage being

492 stopped (Hemes et al., 2019; Kreyling et al., 2021). For the shallow annual mean WTD  
493 registered at our study site we expected lower CO<sub>2</sub> emission according to IPCC Tier 1  
494 emission factors. However, here R<sub>eco</sub> is likely driven by the dynamic interaction of a drop in  
495 WTD during summer coinciding with maximum Ts. This naturally stimulated CO<sub>2</sub>  
496 production in the peat and together with plant respiration drove the high annual R<sub>eco</sub> (Fig 4).  
497 Mean CH<sub>4</sub> emissions from this study were within the range of emissions from pristine and  
498 rewetted Danish and German peatlands reported by Koch et al. (2023) and Tiemeyer et al.  
499 (2020) and no treatment effect was apparent. We found that CH<sub>4</sub> emissions contributed  
500 11.3% to total net mean NECB expressed as CO<sub>2</sub>e (using GWP = 27 for CH<sub>4</sub>). Peatland  
501 rewetting is expected to reduce CO<sub>2</sub> emissions while simultaneously increasing CH<sub>4</sub>  
502 emissions (Abdalla et al., 2016; Darusman et al., 2023). Thus, further monitoring of CH<sub>4</sub>  
503 emissions would be needed as rewetting progresses at the study site.

#### 504 **4.1.2 Management effect on CO<sub>2</sub> emissions**

505 Rewetted nutrient-rich fen peatlands have higher CO<sub>2</sub> emissions compared to low-nutrient  
506 ones (Wilson et al., 2016). Management alternatives to reduce emissions from these sites are  
507 therefore needed in order to meet emission reduction targets. Paludiculture has been found to  
508 effectively reduce emissions from rewetted peatlands (Tanneberger et al., 2020; De Jong et  
509 al., 2021; Bockermann et al., 2024), but type of paludiculture crop seems important for the  
510 reduction potential (Lång et al., 2024). Our results showed that after three years of  
511 establishment and management of RCG at the study site, NECB was not significantly  
512 different compared to no management. These results support findings by Nielsen et al. (2024)  
513 who found no effect of management on GHG emissions during the second year (2020) after  
514 RCG establishment at the study site. The NECB assumes that all harvested biomass is  
515 converted to CO<sub>2</sub> when removed from the field. However, if the biomass is considered as a

516 resource potentially reducing the use of fossil fuels, comparison of NEE among treatments  
517 would also be a relevant measure. Based on NEE, we found a potential emission reduction of  
518 4.5 and 4.7 t CO<sub>2</sub>-C ha<sup>-1</sup> yr<sup>-1</sup> for the 2 and 5-cut management strategies, respectively, in  
519 comparison to no management, but this difference was not significant because of large  
520 variation between treatment replicates especially for the 0-cut. Our NEE estimates were  
521 lower for all treatments compared to Nielsen et al. (2024). We attribute this reduction in net  
522 CO<sub>2</sub> emissions not only to the reduction in biomass production but also to the rewetting  
523 process, which lowered heterotrophic peat mineralization.

524 A life cycle assessment of RCG on fen peatlands by Thers et al. (2023) showed that fuel  
525 consumption during harvesting can make up a considerable amount of GHG emissions  
526 associated to management. Since no considerable difference in yields were found between the  
527 2-cut and 5-cut treatments, and a progressive decline was seen after the third harvest of the 5-  
528 cut treatment, we would recommend the 2-cut management for RCG in peatlands such as the  
529 study site to maximize harvest efficiency and to minimize disturbance to the peatland.

530 Although yields of 2021 (8.9 and 8.6 t DM ha<sup>-1</sup>) (Table A1) were acceptable they were  
531 considerably lower compared to 2019 yields (15.6 and 14.9 t DM ha<sup>-1</sup>) (Nielsen et al., 2021)  
532 and to 2020 yields (12.7 and 13.8 t DM ha<sup>-1</sup>) (Nielsen et al., 2023a) for the 2-cut and the 5-  
533 cut, respectively. The amount of N removed in the harvested biomass was on average 206 kg  
534 N ha<sup>-1</sup> and slightly lower in the 2-cut compared to the 5-cut (Table A2), therefore, the same  
535 amount of N applied as fertilizer was removed at harvest. However, we found generally  
536 higher concentrations of N forms in pore water at the 2 and 5-cut treatments compared to the  
537 0-cut treatment. A complete assessment of the N balance would help to determine the full  
538 environmental benefit of RCG as paludiculture.

#### 539 **4.1.3 Paludiculture and potential CO<sub>2</sub> mitigation**

540 In the most productive blocks of the experiment, paludiculture seemed to accelerate the  
541 reducing effect of rewetting on CO<sub>2</sub> emission. Higher R<sub>eco</sub> and marginally higher NECB were  
542 measured in blocks C and D, which in this study were also the areas with higher porewater  
543 nutrient concentrations compared to R<sub>eco</sub> and NECB measured in the block A. The difference  
544 in emissions between no harvest (0-cut) and harvest (2 or 5-cut) for the highly productive  
545 blocks (C and D) were on average 7.1 t CO<sub>2</sub>-C ha<sup>-1</sup> yr<sup>-1</sup> based on NEE and 2.7 t CO<sub>2</sub>-C ha<sup>-1</sup>  
546 yr<sup>-1</sup> based on NECB. However, in areas of less emissions (block A in this study),  
547 paludiculture would be less recommended because differences were not apparent for  
548 harvested and non-harvested plots and relatively small yields could be harvested as a biomass  
549 resource. These results stress the importance of acknowledging peatland heterogeneity in  
550 rewetting with paludiculture projects to maximize emission reductions.

#### 551 **4.2 Peatland heterogeneity**

552 Even though the studied area was relatively small (3.9 ha) and appeared to be uniform, we  
553 found differences in CO<sub>2</sub> emissions and porewater nutrients among the studied blocks. Peat  
554 chemistry data (Table 1) also indicated differences in pH, organic matter content, and TC  
555 among the studied blocks which might be related to the peat forming process. The peatland  
556 heterogeneity might have originated from differences in topography, groundwater flow, and  
557 vegetation variability, leading to variable rates of peat and C accumulation (Piilo et al., 2020),  
558 and R<sub>eco</sub> (Juszczak et al., 2013). which affected the pore water nutrient concentrations,  
559 microbial communities and GHG balance (Arsenault et al., 2019; Chronakova et al., 2019;  
560 Kou et al., 2020). Mashadi et al. (2024) found, at the same location where this study was  
561 conducted, an increasing degree of peat decomposition approaching the stream, therefore,  
562 higher nutrient concentrations in blocks closer to the stream could be explained by higher  
563 peat decomposition and organic matter mineralization at this area. Heterogeneity at the study  
564 site was also reflected by considerable variability in values of the fitted parameters of the R<sub>eco</sub>

565 and GPP models (Fig 7). Pooling all data to obtain field  $R_{eco}$  and GPP models resulted in  
566 lower model efficiencies (Table A6) compared to the approach of modelling each plot  
567 separately and led to similar  $R_{eco}$ , GPP, and NEE among treatments and blocks (Table A7)..

#### 568 **4.3 Sensitivity of $R_{eco}$ prediction to temporal resolution of WTD**

569 In previous studies, mean annual WTD have been used as the only predictor for NECB, but  
570 not without considerable variation in data points used to build these relationships (Tiemeyer  
571 et al., 2020; Evans et al., 2021; Koch et al., 2023). We found that information on  $T_s$ , RVI and  
572 PAR improved prediction as they have large impact on GPP and  $R_{eco}$ . The other two models  
573 evaluated (models 2 and 3) also included  $T_s$  as explanatory variable. Temperature is a major  
574 soil respiration driver (Silvola et al., 1996; Lafleur et al., 2005; Rigney et al., 2018) as higher  
575 soil temperatures increase microbial activity and soil respiration but it depends also on water  
576 table and soil moisture (Silvola et al., 1996; Lafleur et al., 2005). Out of the three  $R_{eco}$  models  
577 we tested, the combined model including RVI, WTD and  $T_s$  performed best (model 4). When  
578  $R_{eco}$  was estimated by models 2 or 3, where either RVI or WTD was omitted the annual  $R_{eco}$   
579 and thus NECB was underestimated by 8.9 and 3.5%, respectively. Therefore, model  
580 selection is important to accurately estimate  $CO_2$  emissions from peatlands.

581 In this study,  $T_s$  captured major trends in  $R_{eco}$ . This can be seen by the importance of the  
582 fitted  $T_s$  parameter ( $b$ , model 4) (Fig 7) and by results shown in Figure 8, in which hourly  $T_s$   
583 along with mean annual WTD captured most  $R_{eco}$  trends, However, this model  
584 underestimated  $R_{eco}$  by an average of 5%, which would be equivalent to an NECB  
585 underestimation of  $1.2 \text{ t C ha}^{-1} \text{ yr}^{-1}$  compared to the model with hourly WTD and hourly  $T_s$ .  
586 The use of mean annual WTD and mean annual  $T_s$  resulted in an even larger NECB  
587 underestimation ( $3.9 \text{ t C ha}^{-1} \text{ yr}^{-1}$ ) compared to the hourly model. This underestimation is due  
588 to the combined effect of lower WTD and higher  $T_s$  during summer on  $R_{eco}$ , which is not

589 captured when mean WTD and Ts are used. The model based on hourly WTD and Ts also  
590 improved simulation of  $R_{\text{eco}}$  peaks (Figs 8 and A2), which might be of great importance under  
591 extreme weather and climate change conditions. Juszczak et al (2013) also found that the  
592 response of  $R_{\text{eco}}$  to Ts can be influenced by WTD and that models including both WTD and  
593 Ts provide a better representation of  $R_{\text{eco}}$  in heterogeneous peatlands. Emission factors  
594 derived from models based on annual mean WTD, such as those currently used for rewetted  
595 peatlands would underestimate  $R_{\text{eco}}$  when applied to peatlands with fluctuating and lower  
596 WTD during the warm season. This is an important observation particularly for rewetted  
597 peatlands, which might take years to achieve hydrological stability (Kreyling et al., 2021).  
598 Improved  $\text{CO}_2$  modelling therefore requires information on fluctuating WTD possibly  
599 obtained from hydrological modelling if measurement data are unavailable.

#### 600 **4.4 Effect of nutrients in $\text{CO}_2$ emissions**

601 Positive correlations between porewater nutrients suggest common drivers for their release.  
602 Concentrations of dissolved organic matter components have been found to correlate with  
603 concentrations of metals in Canadian bogs (Bourbonniere, 2009). Peat mineralization has  
604 been found to be a major driver of nutrient release from drained peatlands (Cabezas et al.,  
605 2013; Haapalehto et al., 2014). Predominantly higher nutrient concentrations at the studied  
606 blocks compared to the ditch indicate differences between the pore water (measured at the  
607 plots) and the groundwater (measured at the ditch), suggesting that peat mineralization and  
608 fertilization are larger pore water nutrient sources compared to groundwater. Peat nutrient  
609 concentrations and pH have been found to be potential indicators for GHG emissions in  
610 rewetting peatlands (Nielsen et al., 2023b). We showed that the prediction of  $R_{\text{eco}}$  was  
611 improved when soil pore water chemistry data were included in addition to WTD, RVI and Ts  
612 as fixed factors. Although, the magnitude of this improvement was small based on the  $R^2$   
613 increase (between 0.004 and 0.015 depending on the pore water chemistry parameter), this

614 indicated a relation between mineralization and porewater nutrients at the study site. The  
615 exact influence of nutrients on  $R_{eco}$  should be further investigated. In this study we measured  
616 nutrient concentrations but not nutrient load, which is the total mass of a nutrient and can be  
617 more informative about the nutrient status of the peatland (Cabezas et al., 2013). Under  
618 higher (shallower) WTD, nutrient concentrations can be diluted (Griffiths et al., 2019).  
619 Positive correlations between WTD and TOC, DOC and Fe could be due to release of DOC  
620 accumulated under drained summer conditions and increase in Fe solubility under higher  
621 water tables (Haapalehto et al., 2014).

622 Previous studies have explored variability on water chemistry between and within peatlands  
623 (Bourbonniere, 2009; Wood et al., 2016; Arsenault et al., 2018; Griffiths et al., 2019).

624 Nutrient concentrations in peatland's porewater are affected by several factors including  
625 water table depth, temperature, peat decomposition degree, and redox (Bourbonniere, 2009;  
626 Cabezas et al., 2013; Haapalehto et al., 2014; Wood et al., 2016); Furthermore, nutrient  
627 concentrations, base cations, and pH change upon peatland rewetting (Lundin et al., 2017).

628 For this study, WTD was generally lower in blocks C and D (Fig 2B). Malinowski et al.  
629 (2015) found that the area where block A is located is more responsive to changes in the  
630 stream water level due to its proximity to the drainage ditch, which might have caused the  
631 higher mean WTD in this block. Additionally, differences in mobile porosity at the study site  
632 might have made some areas more prone to be affected by changes in WTD than others  
633 (Mashadi et al., 2024). Minor differences in WTD between the replicate blocks could have  
634 produced a different degree of exposure to incoming water sources. Nutrient concentrations  
635 in incoming water sources can in turn affect pore water nutrient concentrations (Bridgham  
636 and Richardson, 1993; Cabezas et al., 2013), which could have contributed to differences  
637 found between blocks, additionally, higher WTD in block A could explain lower nutrient  
638 concentrations due to dilution. The minor differences found in WTD might increase peat

639 mineralization in drier blocks resulting in higher DOC and N concentrations (Arsenault et al.,  
640 2018; Haapalehto et al., 2014; Wood et al., 2016). Nutrient additions have been found to  
641 increase  $R_{eco}$  in peat soils (Larmola et al., 2013). Higher mineralization and larger nutrient  
642 release from organic matter decomposition at lower WTD blocks could explain differences in  
643  $CO_2$  emissions among replicate blocks as evidenced by higher mineralization and  $R_{eco}$  found  
644 at blocks C and D. Higher plant productivity and fresh decomposable organic matter  
645 contributes to higher nutrient concentrations found in rewetted peatlands (Haapalehto et al.,  
646 2014), which could explain higher N concentrations found in blocks C and D. This is also  
647 supported by marginally higher NECB found in these blocks compared to blocks A and B ( $p$   
648  $< 0.1$ ). Nutrients released from the decomposing vegetation have been found to increase soil  
649 respiration and mineralization in high-nutrient peat soils (Larmola et al., 2013). A feedback  
650 mechanism by which higher mineralization and nutrient release enhances plant productivity,  
651 which in turn increases fresh organic matter inputs into the soil and further nutrient releases  
652 could drive high nutrient concentrations in poorly drained fen peatlands such as this one.

#### 653 **4.5 Considerations for the potential use of RCG harvested biomass**

654 In order to reestablish the C sink function of rewetted peatlands, peat formation would need  
655 to be reestablished, however, reaching this state may take decades (Kreyling et al., 2021).  
656 Paludiculture provides an opportunity to achieve indirect GHG emission reductions by  
657 replacing fossil fuels, however, since harvested biomass C makes out a considerable amount  
658 of GHG emissions from cultivated RCG in fen peatlands because it is considered as a  $CO_2$   
659 emission immediately after harvest according to IPCC guidelines (Thers et al., 2023), the end  
660 use of the harvested biomass is key to achieve the potential GHG mitigation. Reed canary  
661 grass grown in wet Danish fen peatlands was shown suitable for protein extraction as  
662 supplement in the diets of monogastric animals and side strips or all the harvested biomass  
663 could be used for biogas production thereby replacing fossil fuels (Kandel et al., 2013);

664 Nielsen et al. 2021; Nielsen et al., 2023a). Since N<sub>2</sub>O was not measured in the present study,  
665 further information is needed to assess the extent of N<sub>2</sub>O contribution to GHG emissions  
666 given that N fertilization for RCG can increase N<sub>2</sub>O emissions in fen peatlands (Kandel et al.,  
667 2019), However, N<sub>2</sub>O emissions equivalent to 1.4 t CO<sub>2</sub>-C was previously reported at the  
668 study site without any difference between harvest and non-harvest treatments (Nielsen et al.,  
669 2024). The feasibility of using biomass from reed canary grass to offset fossil fuels would  
670 depend on the development of non-invasive harvesting techniques, the identification of viable  
671 and economically suitable uses for this biomass, and the establishment of markets and  
672 infrastructure for its processing.

673

## 674 **5. Conclusion**

675 We found that harvesting moderately fertilized RCG in the third production year did not  
676 increase net C emissions significantly in poorly drained fen peatlands compared to no  
677 management. Additionally, a biomass resource that potentially could reduce GHG emissions  
678 elsewhere depending on the end use was produced. When compared with emissions reported  
679 earlier for the second production year, the NECB was further reduced in the third production  
680 year as rewetting progressed. Considering the heterogeneity of the field, results indicate that  
681 harvest of the biomass could potentially reduce net C fluxes at nutrient rich areas, while at  
682 relatively nutrient poor areas it seems more advantageous to leave the grass without  
683 management. Paludiculture and management of RCG in rewetting fen peatlands, therefore,  
684 offers an alternative that could be particularly beneficial in nutrient rich areas. We found that  
685 differences in annual NECB were highly influenced by R<sub>eco</sub>, and that R<sub>eco</sub> was best modelled  
686 by hourly data on RVI, WTD and Ts, with R<sub>eco</sub> being underestimated when the mean annual  
687 WTD was used instead of hourly values, indicating that temporal variability in WTD should

688 be considered in establishing emission factors for rewetted fen peatlands. Differences in  
689 porewater nutrient concentrations were able to further improve prediction of  $R_{\text{eco}}$  based on a  
690 statistical model. As more nutrients could be related to higher  $\text{CO}_2$  emissions, we suggest a  
691 feedback mechanism driving the mineralization, nutrient release, biomass production and  
692 peatland heterogeneity. Further research and the establishment of infrastructure and markets  
693 for harvested biomass would improve the prospects of paludiculture in rewetted peatlands.

694

### 695 **Competing interests**

696 The authors declare that they have no conflict of interest.

697

### 698 **Data availability**

699 Data will be available on Zenodo: <https://doi.org/10.5281/zenodo.14161801>

700

### 701 **Author contributions**

702 PEL designed the experiment, methodology and directed data collection, AFR, JWMP, and  
703 PEL analyzed and visualized the data and wrote the original manuscript, all authors  
704 contributed in revising the manuscript.

705

706 **Acknowledgments** The authors would like to acknowledge the following people from the  
707 Agroecology Department at Aarhus University, Viborg: Michael Koppelgaard for his help in  
708 data collection and processing, Maarit Mäenpää for her help in the statistical analyses,

709 Claudia Nielsen for her help in data processing, and Kirsten Kørup for her help in biomass  
710 harvesting.

### 711 **Funding sources**

712 This study was part of the INSURE project that received funding from the European Joint  
713 Programme EJP Soil under the European Union's Horizon 2020 research and innovation with  
714 grant agreement no. 862695. Co-funding was received from RePeat DK funded by the Danish  
715 Agricultural Agency.

716

### 717 **References**

- 718 Abdalla, M., Hastings, A., Truu, J., Espenberg, M., Mander, Ü., & Smith, P. (2016).  
719 Emissions of methane from northern peatlands: a review of management impacts and  
720 implications for future management options. *Ecology and Evolution*, 6(19), 7080-7102.
- 721 AminiTabrizi, R., Dontsova, K., Grachet, N. G., & Tfaily, M. M. (2022). Elevated  
722 temperatures drive abiotic and biotic degradation of organic matter in a peat bog under oxic  
723 conditions. *Science of the Total Environment*, 804, 150045.
- 724 Andersen, R., Farrell, C., Graf, M., Muller, F., Calvar, E., Frankard, P., ... & Anderson, P.  
725 (2017). An overview of the progress and challenges of peatland restoration in Western  
726 Europe. *Restoration Ecology*, 25(2), 271-282.
- 727 Arsenault, J., Talbot, J., & Moore, T. R. (2018). Environmental controls of C, N and P  
728 biogeochemistry in peatland pools. *Science of the Total Environment*, 631, 714-722.
- 729 Arsenault, J., Talbot, J., Moore, T. R., Beauvais, M. P., Franssen, J., & Roulet, N. T. (2019).  
730 The spatial heterogeneity of vegetation, hydrology and water chemistry in a peatland with  
731 open-water pools. *Ecosystems*, 22, 1352-1367.
- 732 Best, E. K. (1976). An automated method for determining nitrate nitrogen in soil  
733 extracts. *Queensland Journal of Agricultural and Animal Sciences*. 33, 161-166.
- 734 Bianchi, A., Larmola, T., Kekkonen, H., Saarnio, S., & Lång, K. (2021). Review of  
735 greenhouse gas emissions from rewetted agricultural soils. *Wetlands*, 41, 1-7.
- 736 Bockermann, C., Eickenscheidt, T., & Drösler, M. (2024). Adaptation of fen peatlands to  
737 climate change: rewetting and management shift can reduce greenhouse gas emissions and  
738 offset climate warming effects. *Biogeochemistry*, 1-26.
- 739 Bourbonniere, R. A. (2009). Review of water chemistry research in natural and disturbed  
740 peatlands. *Canadian water resources journal*, 34(4), 393-414.

741 Bridgham, S. D., & Richardson, C. J. (1993). Hydrology and nutrient gradients in North  
742 Carolina peatlands. *Wetlands*, 13, 207-218. Cabezas, A., Gelbrecht, J., Zwirnmann, E., Barth,  
743 M., & Zak, D. (2012). Effects of degree of peat decomposition, loading rate and temperature  
744 on dissolved nitrogen turnover in rewetted fens. *Soil Biology and Biochemistry*, 48, 182-191.

745 Cabezas, A., Gelbrecht, J., & Zak, D. (2013). The effect of rewetting drained fens with  
746 nitrate-polluted water on dissolved organic carbon and phosphorus release. *Ecological  
747 engineering*, 53, 79-88.

748 Chroňáková, A., Bárta, J., Kaštovská, E., Urbanová, Z., & Pícek, T. (2019). Spatial  
749 heterogeneity of belowground microbial communities linked to peatland microhabitats with  
750 different plant dominants. *FEMS Microbiology Ecology*, 95(9), 1-130.

751 Crooke, W. M., & Simpson, W. E. (1971). Determination of ammonium in Kjeldahl digests of  
752 crops by an automated procedure. *Journal of the Science of Food and Agriculture*, 22(1), 9-  
753 10.

754 Dansk Standard (2004) DS 291. Water Analyses – orthophosphate-phosphorus. Photometric  
755 method.

756 Darusman, T., Murdiyarsa, D., Impron, & Anas, I. (2023). Effect of rewetting degraded  
757 peatlands on carbon fluxes: a meta-analysis. *Mitigation and Adaptation Strategies for Global  
758 Change*, 28(3), 10.

759 de Jong, M., van Hal, O., Pijlman, J., van Eekeren, N., & Junginger, M. (2021). Paludiculture  
760 as paludifuture on Dutch peatlands: An environmental and economic analysis of Typha  
761 cultivation and insulation production. *Science of the Total Environment*, 792, 148161.

762 Dragoni, F., Giannini, V., Ragaglini, G., Bonari, E., & Silvestri, N. (2017). Effect of harvest  
763 time and frequency on biomass quality and biogas potential of common reed  
764 (*Phragmites australis*) under paludiculture conditions. *BioEnergy research*, 10, 1066-1078.

765 Elsgaard, L., Görres, C. M., Hoffmann, C. C., Blicher-Mathiesen, G., Schelde, K., &  
766 Petersen, S. O. (2012). Net ecosystem exchange of CO<sub>2</sub> and carbon balance for eight  
767 temperate organic soils under agricultural management. *Agriculture, ecosystems &  
768 environment*, 162, 52-67.

769 Emsens, W. J., van Diggelen, R., Aggenbach, C. J., Cajthaml, T., Frouz, J., Klimkowska, A.,  
770 ... & Verbruggen, E. (2020). Recovery of fen peatland microbiomes and predicted functional  
771 profiles after rewetting. *The ISME journal*, 14(7), 1701-1712.

772 Erb, K. H., Kastner, T., Plutzer, C., Bais, A. L. S., Carvalhais, N., Fetzl, T., ... & Luysaert,  
773 S. (2018). Unexpectedly large impact of forest management and grazing on global vegetation  
774 biomass. *Nature*, 553(7686), 73-76.

775 Evans, C. D., Peacock, M., Baird, A. J., Artz, R. R. E., Burden, A., Callaghan, N., ... &  
776 Morrison, R. (2021). Overriding water table control on managed peatland greenhouse gas  
777 emissions. *Nature*, 593(7860), 548-552.

778 Geurts, J. J., Oehmke, C., Lambertini, C., Eller, F., Sorrell, B. K., Mandiola, S. R., ... & Fritz,  
779 C. (2020). Nutrient removal potential and biomass production by *Phragmites australis* and

780 *Typha latifolia* on European rewetted peat and mineral soils. *Science of the Total*  
781 *Environment*, 747, 141102.

782 Giannini, V., Silvestri, N., Dragoni, F., Pistocchi, C., Sabbatini, T., & Bonari, E. (2017).  
783 Growth and nutrient uptake of perennial crops in a paludicultural approach in a drained  
784 Mediterranean peatland. *Ecological engineering*, 103, 478-487.

785 Görres, C. M., Kutzbach, L., & Elsgaard, L. (2014). Comparative modeling of annual CO<sub>2</sub>  
786 flux of temperate peat soils under permanent grassland management. *Agriculture, ecosystems*  
787 *& environment*, 186, 64-76.

788 Griffiths, N. A., Sebestyen, S. D., & Oleheiser, K. C. (2019). Variation in peatland porewater  
789 chemistry over time and space along a bog to fen gradient. *Science of the total*  
790 *environment*, 697, 134152.

791 Haapalehto, T., Kotiaho, J. S., Matilainen, R., & Tahvanainen, T. (2014). The effects of long-  
792 term drainage and subsequent restoration on water table level and pore water chemistry in  
793 boreal peatlands. *Journal of Hydrology*, 519, 1493-1505.

794 Hartung, C., Andrade, D., Dandikas, V., Eickenscheidt, T., Drösler, M., Zollfrank, C., &  
795 Heuwinkel, H. (2020). Suitability of paludiculture biomass as biogas substrate– biogas yield  
796 and long-term effects on anaerobic digestion. *Renewable energy*, 159, 64-71.

797 Hemes, K. S., Chamberlain, S. D., Eichelmann, E., Anthony, T., Valach, A., Kasak, K., ... &  
798 Baldocchi, D. D. (2019). Assessing the carbon and climate benefit of restoring degraded  
799 agricultural peat soils to managed wetlands. *Agricultural and Forest Meteorology*, 268, 202-  
800 214.

801 Jurasinski G, Koebisch F, Guenther A, Beetz S (2022). `_flux`: Flux Rate Calculation from  
802 Dynamic Closed Chamber Measurements. R package version 0.3-0.1, <[https://CRAN.R-](https://CRAN.R-project.org/package=_flux)  
803 [project.org/package=\\_flux](https://CRAN.R-project.org/package=_flux)>.

804 Juszczak, R., Humphreys, E., Acosta, M., Michalak-Galczewska, M., Kayzer, D., & Olejnik,  
805 J. (2013). Ecosystem respiration in a heterogeneous temperate peatland and its sensitivity to  
806 peat temperature and water table depth. *Plant and Soil*, 366, 505-520.

807 Kandel, T. P., Sutaryo, S., Møller, H. B., Jørgensen, U., & Lærke, P. E. (2013). Chemical  
808 composition and methane yield of reed canary grass as influenced by harvesting time and  
809 harvest frequency. *Bioresource technology*, 130, 659-666.

810 Kandel, T. P., Elsgaard, L., & Lærke, P. E. (2017). Annual balances and extended seasonal  
811 modelling of carbon fluxes from a temperate fen cropped to festulolium and tall fescue under  
812 two-cut and three-cut harvesting regimes. *GCB Bioenergy*, 9(12), 1690-1706.

813 Kandel, T. P., Karki, S., Elsgaard, L., & Lærke, P. E. (2019). Fertilizer-induced fluxes  
814 dominate annual N<sub>2</sub>O emissions from a nitrogen-rich temperate fen rewetted for  
815 paludiculture. *Nutrient Cycling in Agroecosystems*, 115, 57-67.

816 Karimi, S., Hasselquist, E. M., Salimi, S., Järveoja, J., & Laudon, H. (2024). Rewetting  
817 impact on the hydrological function of a drained peatland in the boreal landscape. *Journal of*  
818 *Hydrology*, 641, 131729.

819 Kreyling, J., Tanneberger, F., Jansen, F., Van Der Linden, S., Aggenbach, C., Blüml, V., ... &  
820 Jurasinski, G. (2021). Rewetting does not return drained fen peatlands to their old selves.  
821 *Nature communications*, 12(1), 5693.

822 Koch, J., Elsgaard, L., Greve, M. H., Gyldenkerne, S., Hermansen, C., Levin, G., ... &  
823 Stisen, S. (2023). Water table driven greenhouse gas emission estimate guides peatland  
824 restoration at national scale. *Biogeosciences Discussions*, 2023, 1-28.

825 Kou, D., Virtanen, T., Treat, C. C., Tuovinen, J. P., Räsänen, A., Juutinen, S., ... & Shurpali,  
826 N. J. (2022). Peatland heterogeneity impacts on regional carbon flux and its radiative effect  
827 within a boreal landscape. *Journal of Geophysical Research: Biogeosciences*, 127(9),  
828 e2021JG006774.

829 Lafleur, P. M., Moore, T. R., Roulet, N. T., & Frohling, S. (2005). Ecosystem respiration in a  
830 cool temperate bog depends on peat temperature but not water table. *Ecosystems*, 8, 619-629.

831 Larmola, T., Bubier, J. L., Kobyljanec, C., Basiliko, N., Juutinen, S., Humphreys, E., ... &  
832 Moore, T. R. (2013). Vegetation feedbacks of nutrient addition lead to a weaker carbon sink  
833 in an ombrotrophic bog. *Global Change Biology*, 19(12), 3729-3739.

834 Leifeld, J., & Menichetti, L. (2018). The underappreciated potential of peatlands in global  
835 climate change mitigation strategies. *Nature communications*, 9(1), 1071.

836 Leifeld, J., Wüst-Galley, C., & Page, S. (2019). Intact and managed peatland soils as a source  
837 and sink of GHGs from 1850 to 2100. *Nature Climate Change*, 9(12), 945-947.

838 Liu, H., Zak, D., Rezanezhad, F., & Lennartz, B. (2019). Soil degradation determines release  
839 of nitrous oxide and dissolved organic carbon from peatlands. *Environmental Research*  
840 *Letters*, 14(9), 094009.

841 Liu, W., Fritz, C., Weideveld, S. T., Aben, R. C., Van Den Berg, M., & Velthuis, M. (2022).  
842 Annual CO<sub>2</sub> budget estimation from chamber-based flux measurements on intensively  
843 drained peat meadows: Effect of gap-filling strategies. *Frontiers in Environmental*  
844 *Science*, 10, 803746.

845 Loisel, J., & Gallego-Sala, A. (2022). Ecological resilience of restored peatlands to climate  
846 change. *Communications Earth & Environment*, 3(1), 208.

847 Lundin, L., Nilsson, T., Jordan, S., Lode, E., & Strömberg, M. (2017). Impacts of rewetting  
848 on peat, hydrology and water chemical composition over 15 years in two finished peat  
849 extraction areas in Sweden. *Wetlands ecology and management*, 25, 405-419.

850 Lång, K., Honkanen, H., Heikkinen, J., Saarnio, S., Larmola, T., & Kekkonen, H. (2024).  
851 Impact of crop type on the greenhouse gas (GHG) emissions of a rewetted cultivated  
852 peatland. *Soil*, 10(2), 827-841.

853 Malinowski, R., Groom, G., Schwanghart, W., & Heckrath, G. (2015). Detection and  
854 delineation of localized flooding from WorldView-2 multispectral data. *Remote*  
855 *sensing*, 7(11), 14853-14875.

856 Mashhadi, S. R., Grombacher, D., Zak, D., Lærke, P. E., Andersen, H. E., Hoffmann, C. C., &  
857 Petersen, R. J. (2024). Borehole nuclear magnetic resonance as a promising 3D mapping tool  
858 in peatland studies. *Geoderma*, 443, 116814.

859 Nielsen, C. K., Stødkilde, L., Jørgensen, U., & Lærke, P. E. (2021). Effects of harvest and  
860 fertilization frequency on protein yield and extractability from flood-tolerant perennial  
861 grasses cultivated on a fen peatland. *Frontiers in Environmental Science*, 9, 619258.

862 Nielsen, C. K., Stødkilde, L., Jørgensen, U., & Lærke, P. E. (2023a). Ratio vegetation indices  
863 have the potential to predict extractable protein yields in green protein paludiculture. *Mires &*  
864 *Peat*, (29).

865 Nielsen, C. K., Elsgaard, L., Jørgensen, U., & Lærke, P. E. (2023b). Soil greenhouse gas  
866 emissions from drained and rewetted agricultural bare peat mesocosms are linked to  
867 geochemistry. *Science of the Total Environment*, 896, 165083.

868 Nielsen, C. K., Liu, W., Koppelgaard, M., & Lærke, P. E. (2024). To Harvest or not to  
869 Harvest: Management Intensity did not Affect Greenhouse Gas Balances of Phalaris  
870 Arundinacea Paludiculture. *Wetlands*, 44(6), 79.

871 Page, S. E., & Baird, A. J. (2016). Peatlands and global change: response and  
872 resilience. *Annual Review of Environment and Resources*, 41, 35-57.

873 Piilo, S. R., Korhola, A., Heiskanen, L., Tuovinen, J. P., Aurela, M., Juutinen, S., ... &  
874 Väiliranta, M. M. (2020). Spatially varying peatland initiation, Holocene development, carbon  
875 accumulation patterns and radiative forcing within a subarctic fen. *Quaternary Science*  
876 *Reviews*, 248, 106596.

877 Purre, A. H., Penttilä, T., Ojanen, P., Minkkinen, K., Aurela, M., Lohila, A., & Ilomets, M.  
878 (2019). Carbon dioxide fluxes and vegetation structure in rewetted and pristine peatlands in  
879 Finland and Estonia. *Boreal Environment Research*.

880 Putkinen, A., Tuittila, E. S., Siljanen, H. M., Bodrossy, L., & Fritze, H. (2018). Recovery of  
881 methane turnover and the associated microbial communities in restored cutover peatlands is  
882 strongly linked with increasing Sphagnum abundance. *Soil Biology and Biochemistry*, 116,  
883 110-119.

884 R Core Team (2023). *\_R: A Language and Environment for Statistical Computing\_*. R  
885 Foundation for Statistical Computing, Vienna, Austria. <<https://www.R-project.org/>>.

886 Ren, L., Eller, F., Lambertini, C., Guo, W. Y., Brix, H., & Sorrell, B. K. (2019). Assessing  
887 nutrient responses and biomass quality for selection of appropriate paludiculture  
888 crops. *Science of the Total Environment*, 664, 1150-1161.

889 Scharlemann, J. P., Tanner, E. V., Hiederer, R., & Kapos, V. (2014). Global soil carbon:  
890 understanding and managing the largest terrestrial carbon pool. *Carbon management*, 5(1),  
891 81-91.

892 Silvola, J., Alm, J., Ahlholm, U., Nykanen, H., & Martikainen, P. J. (1996). CO<sub>2</sub> fluxes from  
893 peat in boreal mires under varying temperature and moisture conditions. *Journal of ecology*,  
894 219-228.

895 Rigney, C., Wilson, D., Renou-Wilson, F., Müller, C., Moser, G., & Byrne<sup>1</sup>, K. A. (2018).  
896 Greenhouse gas emissions from two rewetted peatlands previously managed for forestry.  
897 *Mires and Peat*, 21, 1-23.

898 Song, Y., Cheng, X., Song, C., Li, M., Gao, S., Liu, Z., ... & Wang, X. (2022). Soil CO<sub>2</sub> and  
899 N<sub>2</sub>O emissions and microbial abundances altered by temperature rise and nitrogen addition in  
900 active-layer soils of permafrost peatland. *Frontiers in Microbiology*, 13, 1093487.

901 Tanneberger, F., Schröder, C., Hohlbein, M., Lenschow, U., Permien, T., Wichmann, S., &  
902 Wichtmann, W. (2020). Climate change mitigation through land use on rewetted peatlands–  
903 cross-sectoral spatial planning for paludiculture in Northeast Germany. *Wetlands*, 40(6),  
904 2309-2320.

905 Thers, H., Knudsen, M. T., & Lærke, P. E. (2023). Comparison of GHG emissions from  
906 annual crops in rotation on drained temperate agricultural peatland with production of reed  
907 canary grass in paludiculture using an LCA approach. *Heliyon*, 9(6).

908 Tiemeyer, B., Freibauer, A., Borraz, E. A., Augustin, J., Bechtold, M., Beetz, S., ... & Drösler,  
909 M. (2020). A new methodology for organic soils in national greenhouse gas inventories: Data  
910 synthesis, derivation and application. *Ecological Indicators*, 109, 105838.

911 Urbanová, Z., & Bárta, J. (2020). Recovery of methanogenic community and its activity in  
912 long-term drained peatlands after rewetting. *Ecological engineering*, 150, 105852.

913 Vroom, R. J., Xie, F., Geurts, J. J., Chojnowska, A., Smolders, A. J., Lamers, L. P., & Fritz, C.  
914 (2018). *Typha latifolia* paludiculture effectively improves water quality and reduces  
915 greenhouse gas emissions in rewetted peatlands. *Ecological engineering*, 124, 88-98.

916 Wilson, D., Blain, D., Couwenberg, J., Evans, C. D., Murdiyarso, D., Page, S., ... & Tuittila,  
917 E. S. (2016). Greenhouse gas emission factors associated with rewetting of organic soils.  
918 *Mires and Peat*, 17, 1-28.

919 Wood, M. E., Macrae, M. L., Strack, M., Price, J. S., Osko, T. J., & Petrone, R. M. (2016).  
920 Spatial variation in nutrient dynamics among five different peatland types in the Alberta oil  
921 sands region. *Ecohydrology*, 9(4), 688-699.

922 Yu, Z., Loisel, J., Brosseau, D. P., Beilman, D. W., & Hunt, S. J. (2010). Global peatland  
923 dynamics since the Last Glacial Maximum. *Geophysical research letters*, 37(13).

924 Zak, D., Roth, C., Unger, V., Goldhammer, T., Fenner, N., Freeman, C., & Jurasinski, G.  
925 (2019). Unraveling the importance of polyphenols for microbial carbon mineralization in  
926 rewetted riparian peatlands. *Frontiers in Environmental Science*, 7, 147.

927 Zambrano-Bigiarini, M. (2020) hydroGOF: Goodness-of-fit functions for comparison of  
928 simulated and observed hydrological time series, R package version 0.4-0. URL  
929 <https://github.com/hzambran/hydroGOF>. DOI:10.5281/zenodo.839854.

930 Zhong, Y., Jiang, M., & Middleton, B. A. (2020). Effects of water level alteration on carbon  
931 cycling in peatlands. *Ecosystem Health and Sustainability*, 6(1), 1806113.

932 Ziegler, R. (2020). Paludiculture as a critical sustainability innovation mission. *Research*  
933 *Policy*, 49(5), 103979.

934 **Appendix A**

935 Table A1. Biomass yields for each harvest event.

treatment	block	Yield per harvest event (t DM ha <sup>-1</sup> )					Total
		20-May	16-jun	04-Ago	14-sep	11-Oct	
2-cut	A	-	2.8	-	1.4	-	4.2
2-cut	B	-	5.3	-	4.8	-	10.1
2-cut	C	-	4.4	-	5.8	-	10.2
2-cut	D	-	4.6	-	6.5	-	11.1
5-cut	A	1.5	1.5	2.9	1.4	0.5	7.8
5-cut	B	1.0	2.6	3.0	1.7	0.5	8.7
5-cut	C	0.3	1.3	3.5	2.1	0.7	7.8
5-cut	D	1.2	1.9	4.2	2.0	0.7	10.1

936

937 Table A2. Total N in harvested biomass per event

treatment	block	total N in biomass per harvest event (kg ha <sup>-1</sup> )					Total
		20-May	16-jun	04-Ago	14-sep	11-Oct	
2-cut	A	-	62	-	31	-	93
2-cut	B	-	104	-	91	-	195
2-cut	C	-	99	-	116	-	215
2-cut	D	-	91	-	113	-	204
5-cut	A	49	38	56	40	21	204
5-cut	B	34	61	65	52	20	233
5-cut	C	13	35	93	74	31	245
5-cut	D	41	47	83	59	27	258

938

939

940

941

942

943

944

945

946

947

948

949

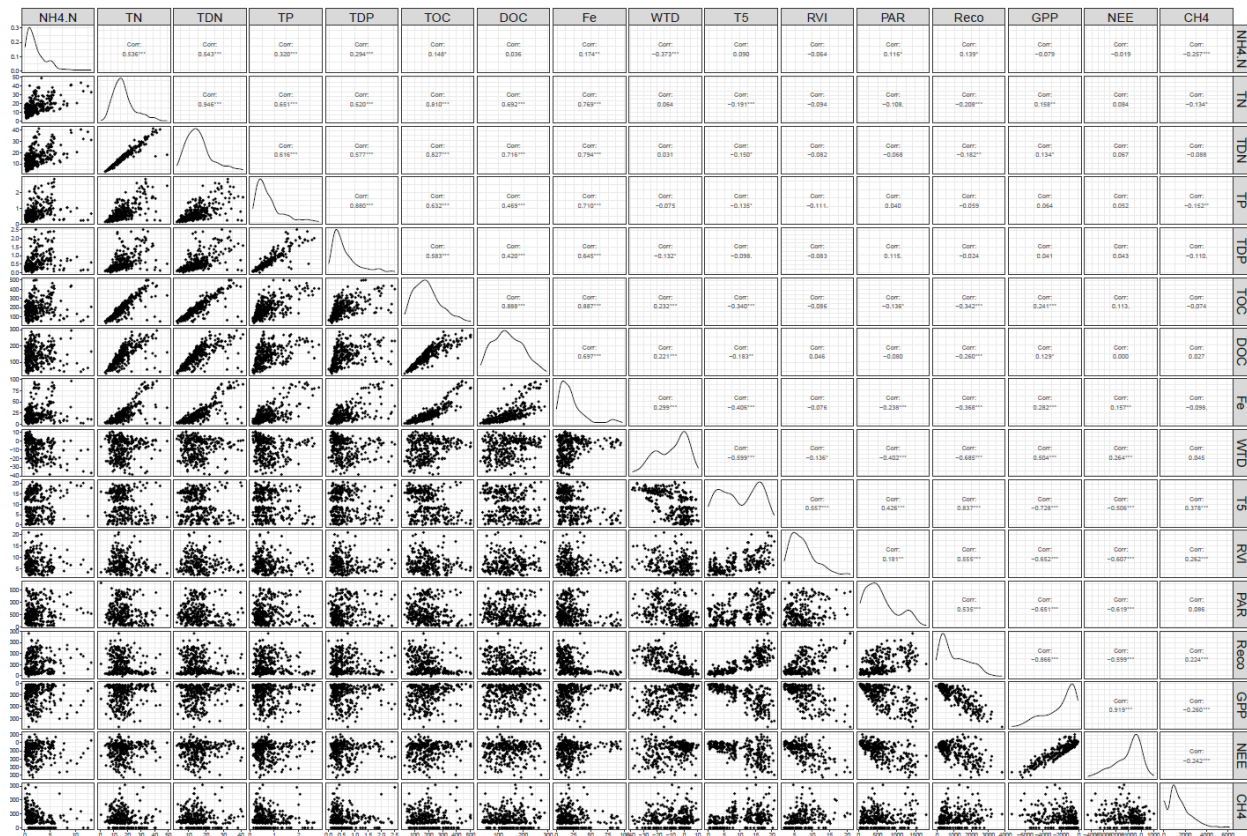
950

951 Table A3. Model evaluation for GPP model. Values are three different indexes of model  
 952 performance for each block.

Block	Treatment	GPP model		
		R <sup>2</sup>	NRMSE	NSE
A	0-cut	0.9	31.1	0.9
	2-cut	0.94	24.2	0.94
	5-cut	0.89	33.9	0.88
B	0-cut	0.91	29.9	0.91
	2-cut	0.96	19.3	0.96
	5-cut	0.94	24.4	0.94
C	0-cut	0.92	27.6	0.92
	2-cut	0.81	43.4	0.81
	5-cut	0.91	30.6	0.91
D	0-cut	0.86	37.5	0.86
	2-cut	0.91	29.3	0.91
	5-cut	0.9	32.4	0.89

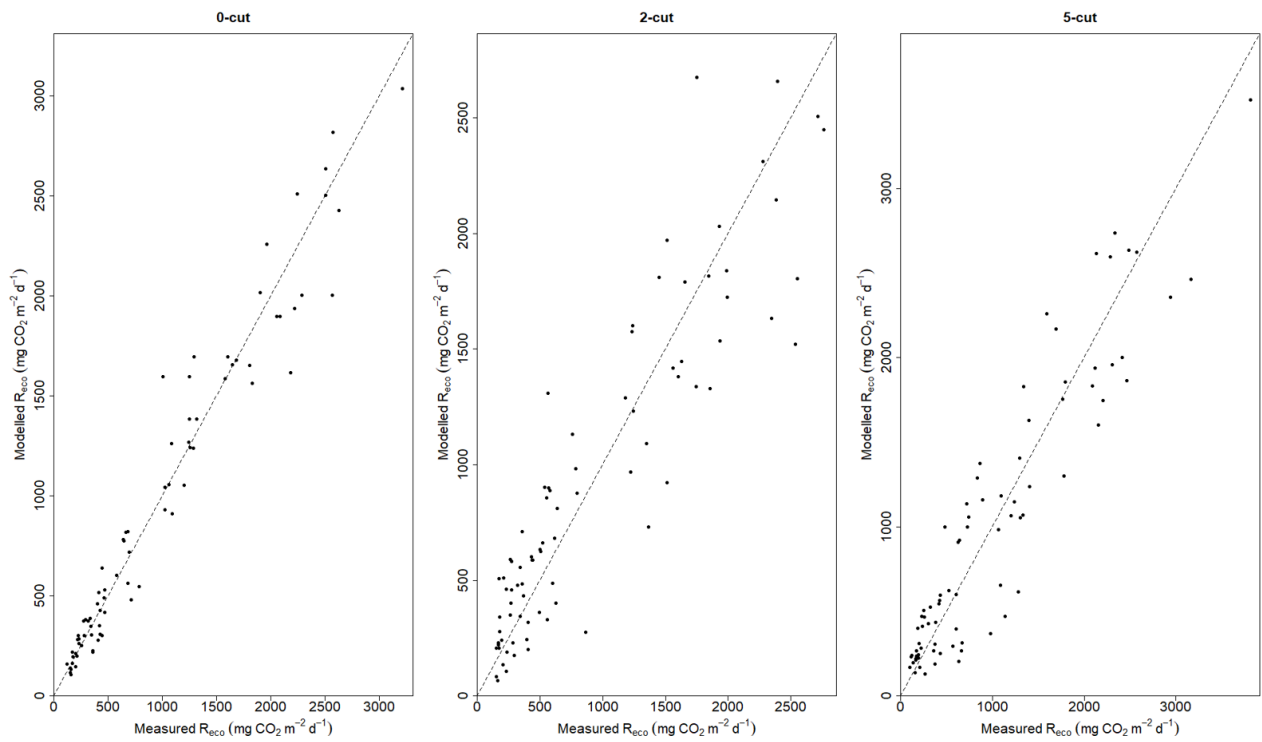
953 A, B, C, and D are the four block replicates, The three harvest treatments at each block are 0,  
 954 2, and 5. The three indexes of model evaluation are: R<sup>2</sup>, normalized root mean square of error  
 955 (NRMSE), and Nash-Sutcliffe efficiency (NSE).

956 Figure A1. Pearson's correlations of water chemistry parameters, Ecosystem respiration  
 957 ( $R_{eco}$ ), net ecosystem exchange (NEE), gross primary productivity (GPP), water table depth  
 958 (WTD), soil temperature at 5 cm depth (T5), ammonia (NH<sub>4</sub>.N), total nitrogen (TN), total  
 959 dissolved nitrogen (TDN), total phosphorus (TP), total dissolved phosphorus (TDP), total  
 960 organic carbon (TOC), and dissolved organic carbon (DOC). \* significant at  $p < 0.05$ , \*\*  
 961 significant at  $0.01 > p > 0.001$  \*\*\* significant at  $p < 0.001$



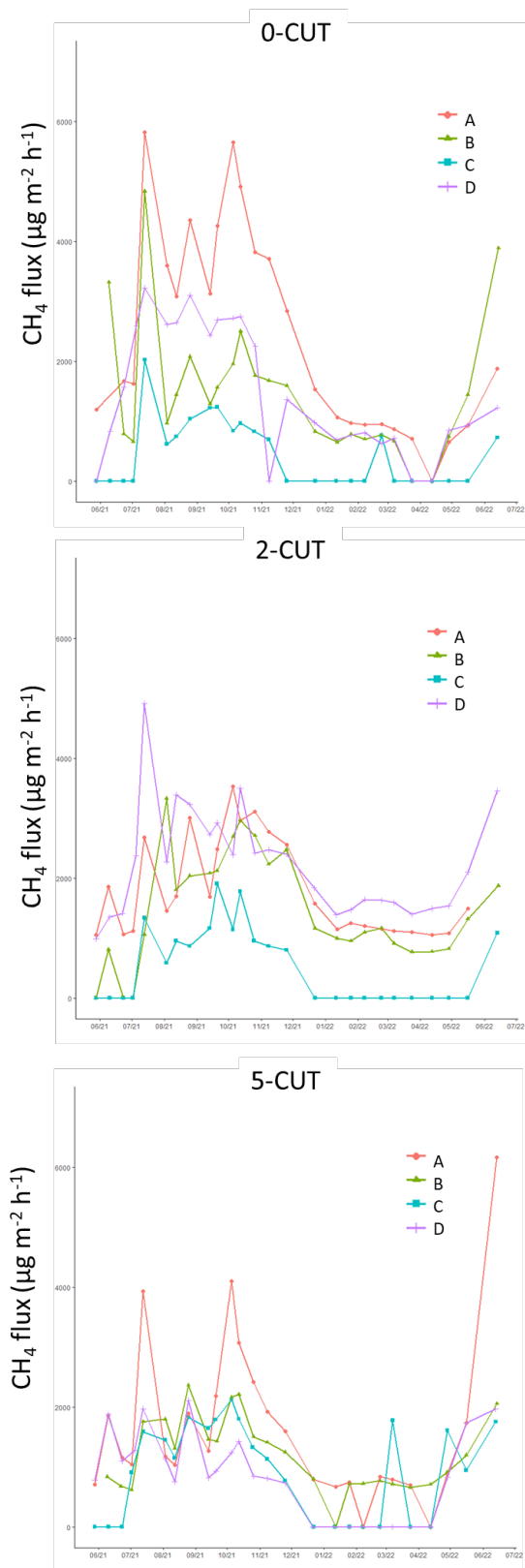
962  
 963  
 964  
 965  
 966  
 967  
 968  
 969  
 970  
 971  
 972  
 973  
 974

975 Figure A2. 1:1 plots of measured vs. modelled Reco using model 4 for the three harvest  
976 treatments. All blocks are included each of the harvest treatments, N = 104.



977  
978  
979  
980  
981  
982  
983  
984  
985  
986  
987  
988  
989  
990  
991  
992  
993

994 Figure A3. Time series of methane emissions from studied blocks (different line colors) and  
995 from the three harvest treatments (zero cut, two cut, and five cut). Each dot in the lines  
996 represents a measurement campaign. CH<sub>4</sub> emissions calculated only under 0% PAR  
997 conditions.



998

999 Table A4. Comparison of annual  $R_{eco}$  estimated with models 4, 2 and 3, which use hourly data  
 1000 on Ts, WTD and RVI, model 4 using either mean annual WTD and Ts (M Model), and model  
 1001 4 using mean annual WTD and hourly Ts (MH model), the latter two models including hourly  
 1002 RVI data.

1003

Block	Treatment	Model 4	Model 2	Model 3	M model	MH model
		t CO <sub>2</sub> -C ha <sup>-1</sup> yr <sup>-1</sup>				
A	0	15.4	14.9	15.4	12.2	14.8
B		18.6	18.4	18.9	14.4	17.7
C		26.2	26.1	25.6	21.6	25.8
D		29.4	29.4	31	25.9	29.4
Average ± SE		22.4 ± 3.3	22.2 ± 3.4	22.7 ± 3.5	18.5 ± 3.2	21.9 ± 3.4
A	2	14.9	14.5	15.1	12.3	13.9
B		23.6	23.4	23.6	20.5	22.4
C		26.4	25.7	26	24.1	24.4
D		23.7	22.7	23	18.7	21.4
Average ± SE		22.1 ± 2.5	21.6 ± 2.4	21.9 ± 2.4	18.9 ± 2.5	20.6 ± 2.3
A	5	20.6	18.6	19.3	17.4	18.6
B		21	20.8	20.5	17.0	19.7
C		23.7	23.6	23.4	19.8	23.4
D		24.3	22.9	23.4	17.9	22.6
Average ± SE		22.4 ± 0.9	21.5 ± 1.1	21.7 ± 1	18 ± 0.6	21.1 ± 1.1

1004

1005 Table A5. Total organic carbon (TOC), dissolved organic carbon (DOC), total nitrogen (TN),  
 1006 total dissolved nitrogen (TDN), total phosphorus (TP), total dissolved phosphorus (TDP),  
 1007 Turbidity (NTU), electrical conductivity (EC). If base model did not improve by adding the  
 1008 water chemistry parameters, R<sup>2</sup> and RMSE are not shown.

1009

Parameter	Reco models				GPP models			
	Base R <sup>2</sup>	Improved R <sup>2</sup>	Base RMSE	Improved RMSE	Base R <sup>2</sup>	Improved R <sup>2</sup>	Base RMSE	Improved RMSE
TOC	0.863	0.873	243	226	-	-	-	-
DOC	0.863	0.871	242	228	-	-	-	-
TN	0.863	0.870	244	229	-	-	-	-
TDN	0.864	0.876	242	224	-	-	-	-
NH <sub>4</sub>	-	-	-	-	-	-	-	-
TP	0.867	0.871	241	231	-	-	-	-
TDP	0.862	0.867	244	229	-	-	-	-
FE	0.863	0.878	242	225	-	-	-	-
pH	0.863	0.868	243	239	0.832	0.839	645	628
NTU	-	-	-	-	-	-	-	-
EC	-	-	-	-	0.832	0.839	643	624

1010

1011 Table A6. Model evaluation of  $R_{eco}$  and GPP models using all data pooled and modelling all  
1012 blocks and harvest treatments all together “field model”

$R_{eco}$ model	$R^2$	0.78
	NRMSE	46.6
	NSE	0.78
	AIC c	14223.49
GPP model	$R^2$	0.88
	NRMSE	34.2
	NSE	0.88

1013 The four indexes of model evaluation are:  $R^2$ , normalized root mean square of error  
1014 (NRMSE), Nash-Sutcliffe efficiency (NSE), and corrected Akaike Information Criteria.

1015

1016 Table A7. Carbon budget results obtained by using all data pooled and modelling all blocks  
 1017 and harvest treatments all together to obtain field models of  $R_{eco}$  and GPP.

Block	Treatment	Reco	GPP	NEE	Yield	NECB
		t CO <sub>2</sub> -C ha <sup>-1</sup> yr <sup>-1</sup>	t CO <sub>2</sub> -C ha <sup>-1</sup> yr <sup>-1</sup>	t CO <sub>2</sub> -C ha <sup>-1</sup> yr <sup>-1</sup>	t C ha <sup>-1</sup> yr <sup>-1</sup>	t C ha <sup>-1</sup> yr <sup>-1</sup>
A	0-cut	21.1	-16.9	4.2	NA	4.2
B		18.8	-15.6	3.2	NA	3.2
C		21.6	-16.6	5.0	NA	5.0
D		23.0	-19.2	3.8	NA	3.8
Mean ±						
SE		21.1 ± 1.6	-17.1 ± 1.3	4.1 ± 0.7	NA	4.1 ± 0.7
A	2-cut	21.9	-17.5	4.4	1.9	6.3
B		22.4	-19.3	3.1	4.5	7.7
C		23.7	-18.4	5.3	4.6	10.0
D		22.1	-16.6	5.5	5.0	10.6
Mean ±						
SE		22.6 ± 0.7	-17.9 ± 1	4.6 ± 1	4 ± 0.7	8.6 ± 1.7
A	5-cut	23.9	-19.4	4.4	3.5	7.9
B		23.7	-20.8	2.9	3.9	6.7
C		25.7	-20.7	5.0	3.5	8.5
D		23.8	-20.3	3.5	4.5	8.0
Mean ±						
SE		24.3 ± 0.8	-20.3 ± 0.6	3.9 ± 0.8	3.8 ± 0.2	7.8 ± 0.7

1018

1019  $R_{eco}$  is ecosystem respiration, GPP is gross primary productivity, NEE is net ecosystem  
 1020 exchange, and NECB of CO<sub>2</sub> is net ecosystem carbon balance (NEE + yield).